



UNIVERSITY OF GENOA

Polytechnic School

**Assessment of offshore wind resources through
measurements from a ship-based LiDAR system**

Thesis for the Master of Science Degree in Environmental and Energy
Engineering

Supervisors

Gabriele Moser
Julia Gottschall

Candidate
Eleonora Catalano

Date
30/03/2017

ACKNOWLEDGMENTS

This thesis is submitted as requirement of the Master of Science “Environmental and Energy engineering” from the University of Genoa and carried out in cooperation with the research institute Fraunhofer IWES Northwest, Germany. This material is based upon work supported by the NEWA funding (by BMWi) and upon data provided by FINO database.

First, I would like to express my sincere gratitude to my supervisors Julia Gottschall and Gabriele Moser, who gave me the opportunity to develop this work and live an invaluable life experience. Thanks a lot to Gerrit Wolken-Möhlmann, Martin Dörenkämper and Bilke Engelbrecht for being always available and for the technical support provided.

Thanks to all the friends I met in Liguria: you made my stay special. Thanks to my cool classmates: Giova, Fabri, Fra, Luca and Davidino. Thanks to the girls: Flavi, for being such an incredible woman and Ali, for all the good times and moments we shared. Thanks to Annina, you always understand me, to Mirko and Renato, for sharing the love for the music with me, and thanks to Cate, for everything you have done for me. Thanks to Ja, Giulia, Rouge, Anto, Fra, Holly and all the guys from Sassello and the Fish&Chips girls for the amazing time we had together and a particular thanks to Najibi, Luchino (vita mia!), Boli, Peppe, Fede, Juliano, Leo, Franklin and all the guys of the campus for the coffees, dinners and great company.

Thanks to Marco Fossa for the chances he gave me and for making my stay in Germany possible. Thanks to all the people I met there: Maria, Julia and Percy for being meine deutsche Familie, thanks to my “best german friends from Jordan” Seif and Ameer, I could not imagine my stay in Bremerhaven without you. Gracias a todos mis amigos latinos, a Ruben, Juan, Juancho, Vale y Susi. Thanks to Hauke, Vivi, Piers and all the guys from 42B, to Helen, Sasha, Jura, Matze and Mr. Swanand for the good time spent together. Thanks to my personal motivator Bilal for his positivity and for the late “Mahlzeit”!

A special thanks to all the friends from Caserta for being always there despite the distance: Merio, Tito, Pab, Stefy, Cacca, Misa, Caccanella, Silvia, Guido, Giovannino, Ada and Davide!

I wish to thank my family, without you all of this would have never been possible. Thank you mom for being such a beautiful example, thanks dad for the love you gave me, I wish you were here with us, and thanks to Federico for being the best and smartest brother of the world.

TABLE OF CONTENTS

Chapter	Page
ACKNOWLEDGMENTS	ii
TABLE OF CONTENTS.....	iv
ABSTRACT.....	vi
SOMMARIO	vii
LIST OF TABLES	ix
LIST OF FIGURES	x
LIST OF ABBREVIATIONS.....	xiii
NOMENCLATURE	1
INTRODUCTION	2
1. CHAPTER I: LITERATURE REVIEW.....	4
1.1 Wind resource assessment.....	4
1.1.1. History and purpose	4
1.1.2. Wind resource maps.....	6
1.1.3. Challenges.....	7
1.2. LIDAR: remote sensing of wind by light.....	9
1.2.1. Introduction to lidar	9
1.2.2. Wind lidars.....	10
1.2.3. Applications for wind energy	12
1.3. Ship-lidar measurements.....	14
1.3.1. Introduction.....	14
1.3.2. Fields of application and challenges	14
1.4. Data sources for validation and verification	16

2.	CHAPTER II: METHODOLOGY	23
2.1.	Ship-lidar data as an offshore wind resource assessment	23
2.1.1.	Projects and measurement campaigns	24
2.2.	Ship-lidar system.....	27
2.2.1.	Measurement principle	27
2.2.2.	Motion influence on ship-based lidar measurements	28
2.2.3.	Complete motion correction	30
2.2.4.	Simplified motion correction.....	31
2.3.	Ship-lidar verification and comparison.....	33
2.3.1.	FINO1 campaign: FINO1-Lidar comparison	34
2.3.2.	Helgoland campaign: DWD-Lidar comparison.....	38
2.3.3.	Helgoland campaign: WRF-Lidar comparison.....	40
3.	CHAPTER III: RESULTS AND DISCUSSION.....	47
3.1.	Results and assessment	47
3.1.1.	Post-processing procedure and example dataset from the Helgoland campaign.....	48
3.1.2.	Results and assessment of the Helgoland campaign.....	52
3.1.3.	Results, assessment and sensitivity for the FINO1 campaign	63
3.1.4.	Discussion on usability and feasibility of the final approach	68
3.2.	Outlook and future research work.....	69
	CONCLUSIONS	70
	REFERENCES	72
	Appendix A – Results of the Helgoland campaign.....	75
	Appendix B – Results for the FINO1 campaign.....	82

ABSTRACT

As the wind farm industry is constantly growing, the assessment of the wind energy resource is fundamental for the evaluation of the feasibility of wind farm projects. Offshore projects require high investment and installation costs and therefore an accurate wind estimation method is necessary in order to guarantee the bankability of the project. Nowadays, offshore measurements are realized by means of meteorological (met.) masts, which implies very high costs and possible constructional restrictions, and lidar (Light Detection and Ranging) buoys, which represent a more flexible and cost-efficient alternative but operate on fixed locations and might be difficult to maintain reliably.

The Fraunhofer Institute for Wind Energy and Energy System Technology (IWES) has recently developed a ship-based lidar system. Unlike the aforementioned buoy-based systems, not only it allows wind characteristics to be measured, but it also provides measurements in both space and time, exploiting the already existent track of a given ship, and is substantially more convenient to maintain. Nevertheless, the ship velocity and rotational movements influence the recorded data and therefore need to be considered and corrected.

The scope of this thesis is to evaluate the applicability of the ship-lidar system and the reliability of possible correction methods. An approach for processing the data is developed and validated through two campaigns, namely FINO1 and Helgoland. Outcomes of the comparison with FINO1 data are characterized by very high coefficients of determination. Regarding the Helgoland campaign, a preliminary comparison with meteorological datasets points out a good agreement between the two data sources. A further outcome of the thesis is the routine for the comparison of lidar and weather simulation from the WRF model: this comparison shows a good fit as well, although it is limited by the possible inaccuracies of the simulation itself.

In conclusion, a ship-based system results to be a good solution compared to the conventional measurement choices, especially for short-period measurements in areas that are covered by already existing available vessel tracks.

SOMMARIO

Con la crescita dell'industria delle *wind farm*, la stima della disponibilità e della distribuzione delle fonti di energia eolica è sempre più fondamentale per la valutazione della fattibilità di realizzazione di un impianto eolico. I progetti *offshore* richiedono infatti elevati investimenti e costi di installazione, quindi metodologie accurate di stima del vento risultano necessarie al fine di valutare e garantire la fattibilità economica di un progetto. Attualmente, le misurazioni *offshore* relative al campo di velocità del vento sono tipicamente realizzate tramite *met. mast* (torri di misurazione meteorologiche), le quali implicano alti costi e possibili restrizioni costruttive, e *boe lidar* (*Light Detection and Ranging*), che rappresentano un'alternativa più flessibile ed efficiente ma operano in posizioni prefissate e possono presentare difficoltà di manutenzione.

Il *Fraunhofer Institute for Wind Energy and Energy System Technology* (IWES) ha recentemente sviluppato un sistema lidar installato su una nave. A differenza dei sopraccitati sistemi lidar installati su *boe*, esso consente non solo di misurare le caratteristiche di velocità del vento ma anche di fornire tali misurazioni nello spazio e nel tempo, sfruttando la rotta già esistente di una nave e consentendo una manutenzione più conveniente. Tuttavia, la velocità della nave ed i suoi moti rotazionali influenzano i dati registrati, che pertanto devono essere corretti.

Lo scopo di questa tesi è valutare l'applicabilità del sistema nave-lidar sviluppato e l'affidabilità dei relativi metodi di correzione dei dati. Un approccio per elaborare i dati è stato qui sviluppato e validato sperimentalmente attraverso due campagne di misurazione, chiamate FINO1 e Helgoland. I risultati del confronto fra le stime di velocità del vento ottenute dall'approccio proposto e le misurazioni *in situ* relative alla campagna FINO1 sono caratterizzati da valori molto elevati di coefficiente di correlazione. Per quanto riguarda la campagna Helgoland, un confronto preliminare con dati meteorologici mostra una correlazione abbastanza elevata tra le due sorgenti di dati. Un ulteriore esito della tesi è anche un modello per il confronto tra dati di vento estratti mediante lidar e mediante simulazioni meteo (WRF): esso ha permesso di verificare che le due sorgenti informative siano abbastanza concordi, anche se con limitazioni dovute a possibili imprecisioni della

simulazione stessa.

In conclusione, il sistema nave-lidar si rivela essere una soluzione efficace in confronto ad i sistemi di misura convenzionali, specialmente per misurazioni di breve durata in aree già coperte da preesistenti rotte navali.

LIST OF TABLES

Table	Page
Table 1.1: Comparison among different wind data sources.	22
Table 3.1: influence of the time step chosen for the lidar mean on the resulting coefficient of determination.	62
Table 3.2: results from lidar-WRF comparison for 30-min mean lidar values. The first column shows the time of the day taken into account for the comparison; the second shows the number of data selected and the third one the corresponding coefficient of determination.	62
Table 3.3: results from data assessment for lidar measurements of wind speed in the FINO1 campaign.	65

LIST OF FIGURES

Figure	Page
Figure 1.1: Two wind lidars: pulsed lidar and continuous wave (CW) (©ZephIR/Leosphere) [21].....	11
Figure 1.2: Offshore met. mast FINO1 in the North Sea at the location N54 00' 53,5" E 6 35' 15,5".....	17
Figure 1.3: Fraunhofer IWES wind lidar buoy [2].	19
Figure 1.4: The diagram shows the main ocean wind satellite technology types, their spatial and temporal resolutions, and their main application domains [12].....	20
Figure 2.1: Lidar and sensor box installed in the frame, fixed to the top deck of the LEV Taifun [14].	24
Figure 2.2: LEV Taifun during measurement campaign in proximity to FINO1 [16].	25
Figure 2.3: Map showing the start and end locations of the ship route in the two red circles	26
Figure 2.4: Schematic of the velocity–azimuth display scanning [22].....	28
Figure 2.5: Data flow of the different correction algorithms [11].	29
Figure 2.6: Extract of map showing offshore wind parks in the German Bight with the location of FINO1 marked red.	35
Figure 2.7: Ship track in proximity to FINO1 [16].....	35
Figure 2.8: Wind speed deviation (lidar – FINO1) at 100 m versus wind direction at 90 m.	36
Figure 2.9: Wind speed deviation (lidar – FINO1) versus reference wind direction at 60 m.	37
Figure 2.10: The port of Bremerhaven with the position of the ferry and the met. mast.	39

Figure 2.11: The port of Helgoland with the position of the ferry and the met. mast.	39
Figure 2.12: Arakawa grid of WRF models.	40
Figure 2.13: Interpolation from pressure levels η to measurement height z_0 [2].....	43
Figure 2.14: Route of the ship from Bremerhaven to Helgoland and way back.	44
Figure 2.15: Route of the ship from Bremerhaven to Helgoland and way back on July 3 (non-interpolated samples).	45
Figure 3.1: Comparison between corrected and uncorrected wind speed.	48
Figure 3.2: Comparison between corrected and uncorrected wind direction for the selected day.....	49
Figure 3.3: Corrected lidar data for 03 August 2016 and three different heights.....	50
Figure 3.4: Wind speed trend for the whole month of July 2016 at 100 m height.	51
Figure 3.5: Comparison between the ship-lidar wind speed and the DWD wind speed time series.	52
Figure 3.6: Comparison between the ship-lidar wind direction and the DWD wind direction values.	53
Figure 3.7: Comparison between the ship-lidar and the DWD wind speed and direction, respectively.	54
Figure 3.8: Difference between lidar wind speed and WRF wind speed.	55
Figure 3.9: Coordinate of the ship plotted over time for the day 3 July 2016.	56
Figure 3.10: Wind speed over time for 3 July 2016.	57
Figure 3.11: wind speed over time for 1 and 10 July 2016..	58
Figure 3.12: Correlation plots for wind speed values obtained by the lidar measurements and the WRF simulation.	59
Figure 3.13: Correlation plot between 30-min average wind speed from lidar measurements and the WRF simulation.	60

Figure 3.14: correlation between 30-min average wind speed from lidar measurements and the WRF reference.	61
Figure 3.15: Wind speed for the sample day 11 June 2014.	63
Figure 3.16: Wind direction for the sample day 11 June 2014.	64
Figure 3.17: Correlation plot for measurements of horizontal wind speed at 100 m.	65
Figure 3.18: Correlation plot for measurements of horizontal wind speed at 60 m.	66
Figure 3.19: Sensitivity study: difference between the wind speed measured by lidar and the reference speed measured by the sensor at 100 m versus the ship speed.	67
Figure 3.20: Sensitivity study: difference between the wind speed measured by lidar and the reference speed measured by the sensor at 100 m versus distance from FINO1.	67
Figure A.1: Wind speed trend for the whole month of June 2016 at 100 m height.	75
Figure A.2: Wind speed trend for the whole month of August 2016 at 100 m height.	76
Figure A.3: Wind speed over time for the days 2 and 5 July 2016.	76
Figure A.4: Wind speed over time for the days 6 – 7 – 8 – 9 – 11 – 12 July 2016.	77
Figure A.5: Wind speed over time for the days 13 – 14 – 15 – 16 – 17 - 18 July 2016.	78
Figure A.6: Wind speed over time for the days 19 – 20 – 21 – 22 – 23 – 24 July 2016.	79
Figure A.7: Wind speed over time for the days 25 – 26 – 27 – 28 – 29 – 30 July 2016.	80
Figure A.8: Wind speed over time for day 31 July 2016.	81
Figure B.1: Wind speed for the sample day 12 June 2014.	82
Figure B.2: Wind speed for the sample day 31 June 2014.	83
Figure B.3: Wind speed for the sample day 14 June 2014.	84

LIST OF ABBREVIATIONS

WRA	Wind Resource Assessment
LiDAR	Light Detection and Ranging
WPP	Wind Power Plant
AEP	Annual Energy Production
NEWA	New European Wind Atlas
RS	Remote Sensing
LoS	Line of Sight
LSE	System of Linear Equations
LAT	Lowest Astronomical Tide
WRF	Weather Research Forecast
EERA-DTOC	European Energy Research Alliance - Design Tool for Offshore Wind Farm Cluster
VAD	Velocity-Azimuth Display
AHRS	Attitude and Heading Reference Sensor
DWD	German Weather Service
FLS	Floating Lidar System
IWES	Institute for Wind Energy and Energy System Technology
SAR	Synthetic Aperture Radar

NOMENCLATURE

Symbol	Meaning	Units
u_{NS}	wind speed in the north–south direction	[m/s]
u_{EW}	wind speed in the east–west directions	[m/s]
O_{till}	tilted beam orientation matrix	[-]
u	wind speed	[m/s]
$u_{measured}$	wind speed measured from the lidar	[m/s]
u_{system}	ship velocity	[m/s]
$R_{yaw,pitch,roll}$	rotation matrix for one point in time	[-]
HGT	height	[m]
d	distance	[m]
PH	geopotential	[m ² /s ²]
PHB	base-state geopotential	[m ² /s ²]
t	time	[s]
R ²	coefficient of determination	[-]
Greek letters		
θ	center of the cell	[-]
η	pressure level	[hPa]
θ	wind direction	[deg]
\emptyset	half-opening angle	[deg]

INTRODUCTION

Wind energy is now one of the fastest-growing renewable energy sources and resource assessment for this source is fundamental for the planning of wind energy projects. A detailed knowledge about site-specific environmental conditions allows to better evaluate the feasibility and profitability of a wind farm, especially in terms of costs and investments. Since wind energy competes with fossil fuels for the production of electricity, it needs to be convenient enough and its assessment needs to have as small uncertainty as possible. Therefore, the results of the measurement should be precise, and detailed and have to represent the true conditions.

In particular, offshore projects require high investment costs and include both the big-scaled turbines and the connections to the mainland that have to transfer the energy produced. In order to guarantee the bankability of an offshore wind project, many wind resource estimation methods have been developed and used, and they are continuously improving as the fast growth of the wind-farm industry requires.

Nowadays, both onshore and offshore measurements are mainly realized by means of meteorological (met.) masts and lidar (Light Detection and Ranging) buoys. In addition, satellite observations are a useful data source although it offers a sparser time sampling. Offshore, the installation of met. masts is associated with very high costs and possible constructional restrictions, while the lidar systems represent a more flexible and cost-efficient alternative. A lidar buoy has been developed by the Fraunhofer Institute for Wind Energy and Energy System Technology (IWES) and made for a substantial reduction of costs and uncertainties for offshore campaigns. However, even the lidar buoy is subject to failures of single components that, especially in situations where the weather conditions make the required maintenance difficult, lead to gaps in measurement time series.

To overcome these drawbacks, a new measurement system has been developed and tested: the ship-based lidar system. It does not only allow to measure wind characteristics without addressing these problems, but it also provides measurements in both space and time, thus exploiting the already existent track of a given ship.

The scope of this thesis is to evaluate the applicability of this measurement system and the reliability of the possible correction methods to be applied to the recorded lidar data. Indeed, since the ship is moving, a correction of the data is necessary, otherwise the data would be severely biased by the motion of the platform. Within the thesis, two measurement campaigns carried out in the North Sea are considered, correction algorithms for the ship-based lidar measurements of wind speed are developed, and the resulting wind speed measurements are evaluated and compared with reference sources, including the met. mast FINO1 in the first campaign and the met. masts in the ports of Bremerhaven and Helgoland during the second campaign. As a further validation step, the wind speed measurements collected using the proposed approach are compared with the results of the Weather Research Forecasting (WRF) simulation model, which allows further insight in the property of the developed wind speed product to be understood.

The thesis is structured as follows: Chapter 1 recalls the related background information and presents a literature review about wind resource assessment, wind lidars, ship-based lidar measurements, and wind data sources. Chapter 2 focuses on the proposed approach to wind-speed measurement: it describes the measurement campaign and the ship-lidar system in details, the motion correction methods, and the ship-lidar verification and comparison methodology. In Chapter 3, the results are showed and discussed in detail, and possible improvements and future research work are mentioned. Finally, conclusions on the main outcomes of this research work are drawn. Appendices A and B show all the results for both considered campaigns.

1. CHAPTER I: LITERATURE REVIEW

1.1 *Wind resource assessment*

1.1.1. History and purpose

Wind is widely recognized as a clean source of energy and is a sustainable option in the pursuit of renewable energy. Moreover, since the wind is a free resource, once a turbine is erected the only costs that need to be considered are operational and maintenance costs. The input raw material (feedstock) for a wind power plant (WPP) is wind; therefore, there is no pollution or environmental degradation due to the mining and/or transporting of raw materials like coal, crude oil, or natural gas. The output is clean electricity with absolutely no pollutants (e.g., no carbon dioxide, sulfur oxides, nitrogen oxides, or mercury compounds) and the WPP does not use water. All these characteristics of WPPs provide significant tangible benefits in terms of improved health and conservation of natural resources.

Because of this consideration, wind power is currently the fastest-growing renewable energy worldwide. In countries with viable wind resources, deployment of wind power features prominently in the renewable energy road map. A crucial activity during the development phase of a wind project is wind resource assessment (WRA).

WRA quantifies the wind resource and represents the most important step in planning a community wind project. It is not only the basis for determining initial feasibility and cash flow projections, but it is also fundamental to map the wind resources for a region or a country. Modern wind resource assessments have been conducted since the first wind farms were developed in the late 1970s. Developers and researchers in Denmark, where the modern wind power industry first developed, pioneered the methods used.

When developing wind energy markets, it is important to encounter bankable WRAs that meet international standards with respect to:

- on-site wind measurement with tall towers and high-quality instruments for a period of at least 1 year;
- auditable data acquisition, processing, and archiving;
- rigorous modeling of wind flow based on a linear model for simple terrain and a computational fluid dynamics model for complex terrain;
- credible estimate of losses and uncertainties.

As a drawback, a poorly executed WRA that does not meet international standards can significantly increase the lead-time of the wind project, for example, from 2 years to over 5 years. In such cases, in addition to the delay, the developer is forced to invest additional capital. A strong and committed developer may continue with more investment, but large fraction of financially weak developers choose to abandon projects, even though these projects hold development licenses and land concessions [3].

Recommended strategies to assist developers and increase chances of success for wind projects in the development phase include, for example, to offer grants or low-interest loans to qualified developers with strict conditions that pertain to the use of best practices for bankable WRAs. In addition, to create licensing guidelines that clearly state conditions on the quality of WRAs prior to issuing a generation license can help pursuing this purpose. A further point can be to develop capacity of developers through knowledge transfer and training in order to make their job more efficient and, finally yet importantly, a good strategy is to develop long-term wind measurement campaigns to collect high-quality long-term wind data. All these possibilities lead to a higher probability that the projects under development are financed and subsequently built.

The resulting output of a bankable WRA is the average annual energy production (AEP), the net AEP after losses and the uncertainty associated with net AEP. This is used in the financial analysis of the project, with uncertainty playing a prominent role, and to determine the viability of a wind project; hence, during the development stage, strong due diligence must be exercised in order to minimize uncertainties due to measurement, modeling, and other factors.

1.1.2. Wind resource maps

The Wind Atlas is a wind resource map containing data on the wind speed and wind direction in a specific region. These data include not only maps but also wind speed and direction time series or frequency distributions. Therefore, the main objectives of a wind atlas are to provide wind resource data accounting for high-resolution effects, use microscale modelling to capture small-scale wind speed variability (crucial for better estimates of total wind resource), use a unified methodology and verify the results in representative selected areas.

In some countries, government agencies publish maps of estimated wind resources that serve to inform policy-making and encourage wind power development. Examples include the Canadian Wind Atlas, the European Wind Atlas, and the Wind Resource Atlas of the United States. In particular, areas potentially suitable for wind energy applications are available throughout all the European countries. Major areas that have a high wind energy resource include Great Britain and Ireland, the northwestern continental parts of the European Union (EU): Denmark, northern Germany, the Netherlands, Belgium and northwestern France. Other areas are northwestern Spain and a majority of the Greek islands. In addition, there are many areas, in particular in the Mediterranean countries, where wind systems associated with mountain barriers give rise to high-energy potentials, e.g. the Mistral between the Alps and the Massif Central in the south of France, the Tramontane north of the Pyrenees in France and south of the Pyrenees in the Ebro valley. In other cases, such wind systems are of smaller geographical extent but may give a large wind resource locally [5].

The European Wind Atlas is divided into three parts, each intended for readers with different areas of interest - from nonprofessionals to professional meteorologists.

The first part provides an overall view of the wind climate and magnitude and distribution of wind resources in the European countries. This part of the Atlas is intended to be useful to politicians, planners, and nonprofessionals in general. The descriptions, tables, and maps permit a first, rapid identification of regions with favorable wind resources.

The second part gives explanations and information needed for the purpose of regional wind resource assessments and the local siting of wind turbines. It contains the raw statistics for

meteorological stations, the regional climatological statistics and includes methods for calculating the influence on the wind resource of various features in the landscape such as coastlines, forests, hills, and buildings. Examples are given both for relatively uncomplicated conditions where the methods and statistical tables can be used directly and for conditions where the calculations have been performed on a personal computer. These examples are produced with a programme specially developed with this intent: the Wind Atlas Analysis and Application Programme (WASP).

The third and last part is the documentation part of the Atlas. It describes how the analysis was performed from the data and the information gathered by each participating country to the resulting regional climatological statistics. Furthermore, the validity of the models and the analysis is demonstrated through a number of comparisons between measured and modelled wind statistics [5].

Although the accuracy has improved, it is unlikely that wind resource maps, whether public or commercial, will eliminate the need for on-site measurements for utility-scale wind generation projects [6]. However, mapping can help speed up the process of site identification and the existence of high quality, ground-based data can shorten the amount of time that on-site measurements need to be collected.

1.1.3. Challenges

A New European Wind Atlas (NEWA) is the next step of the research and development activities in this field. The main objective of NEWA is the development of a New European Wind Atlas and the improvement of advanced models towards the reduction of uncertainties to less than 3% for flat homogenous terrains and the strategic key performance indicator for “Resource assessment and spatial planning” of the European Industrial Initiative on wind energy [4].

The overall goal of the NEWA project has several technological and scientific objectives:

- development of a high-value data bank from a series of wind measurement campaigns;
- development of methodology and improvement of advanced models for wind farm development, wind turbine design conditions, spatial planning, and policy promotion;
- creation and publication of a European Wind Atlas;
- verification and estimation of uncertainty.

In the context of this project, this thesis contributes to the offshore area of the North Sea. Furthermore, in addition to wind resource information, the new Atlas will give measures of wind variability, wind power predictability from day-ahead to decadal as well as parameters for wind turbine design.

1.2. LIDAR: remote sensing of wind by light

1.2.1. Introduction to lidar

Lidar (also called LIDAR, LiDAR, and LADAR) is a surveying method that measures distance to a target by illuminating that target with a laser light. The name lidar was originally a portmanteau of light and radar, although nowadays is mainly considered as an acronym of Light Detection And Ranging (sometimes Light Imaging, Detection, And Ranging). Lidar originated in the early 1960s, shortly after the invention of the laser, and combined laser-focused imaging with the ability to calculate distances by measuring the time for a signal to return using appropriate sensors and data acquisition electronics. Lidar has been used extensively for atmospheric research and meteorology; in fact, the National Center for Atmospheric Research used it for the first time to measure clouds [7].

Lidar uses ultraviolet, visible, or near infrared light to image objects. It can target a wide range of materials, including non-metallic objects, rocks, rain, chemical compounds, aerosols, clouds, and single molecules. The light return is typically originated via backscattering and different types of scattering are used depending on lidar applications: most commonly Rayleigh scattering, Mie scattering, Raman scattering, and fluorescence. Suitable combinations of wavelengths can allow for remote mapping of atmospheric contents by identifying wavelength-dependent changes in the intensity of the returned signal.

Lidar has a wide range of applications that can be divided into airborne, when it is used to create a 3D point cloud model of the landscape while it is attached to a plane or drone during flight, and terrestrial types, which happen on the Earth's surface and can be either stationary or mobile. Mobile lidar is a system in which two or more scanners are attached to a moving vehicle to collect data along a path and are coupled with a satellite navigation system. These different types of applications require scanners with varying specifications based on the purpose of the data, the size of the area to be captured, the range of measurement desired, the cost of equipment, and more.

1.2.2. Wind lidars

Today, the rate of wind turbines are being installed on, offshore, in hilly and forested areas, and even in complex or mountainous terrain is continuously increasing. At the same time, as the turbines gets bigger and more powerful, they also reach higher and higher into the atmospheric flow, and thereby also into hitherto unknown wind and turbulence regimes - on as well as offshore. Because of this growth, the traditional single accurately calibrated cup anemometer installed at hub height used for performing traceable measurements is becoming more cumbersome and expensive. Furthermore, as wind turbines rotor planes reaches 120 m in diameter or more it is evident that the incoming wind field over the entire rotor planes is not measured representatively from a single cup anemometer mounted at hub height. Thus, research activities are working towards the establishment of new research infrastructure based on wind lidars.

Remote Sensing (RS) measurement methodologies for wind energy applications are today commercially available and the application range for wind measurements are also plentiful, and encompass for example:

- Wind turbine power performance verification – establishment of new RS based measurement standards for the replacement of in-situ reference met masts;
- Wind energy resource measurements – the global wind resources are now being mapped globally on shore, off shore, over hilly and in mountainous terrain, etc. Here as well, high accuracy is of uttermost importance for accurate site and resource assessments;
- Wind turbine control – RS lidar instruments that are directly integrated into the wind turbine hub or spinner or even into the blades are also seen as a forthcoming RS measurement technology that can help improving the wind turbines power performance [8].



Figure 1.1: Two wind lidars: pulsed lidar and continuous wave (CW) (©ZephIR/Leosphere) [21].

As it is possible to see from Figure 1.1, wind lidars in the market for vertical mean and turbulence profile measurements are available based on two different measurement principles:

1. Continuous wave (CW) lidars - continuously transmit a light beam and analyze the backscatter by using the Doppler shift;
2. Pulsed lidars - transmit sequences of light pulses and then determine the Doppler shift in the backscattered light of each pulse.

CW lidars measure the wind vector of each height successively by adjusting the focus of the optical telescope according to predefined measurement heights or ranges. At each range, the wind vector typically is conically scanned. The radial wind speed at the respective heights is determined by applying a weighting function to the measured frequency shifts. Particles that are close to the focusing range where the beam has the greatest intensity are weighted the most while those, which are further away, are weighted less. While the minimum range of the telescope depends on its focus capabilities, the capability of each telescope to focus

decreases with an increasing distance from the lens. The vertical resolution of the system thus limits the maximum measurement height of CW lidars. Therefore, they are considered as short-range devices. Recent systems are able to measure the wind vector at heights from 10 m up to 200 m [8, 9].

Pulsed lidar systems measure the wind speed at up to more than ten ranges or range-gates simultaneously by determining the arrival time of a light pulse. The time delay between the pulse start and the measurement time informs on the distance of the analyzed zone. Contrarily to CW lidars, the maximum measurement height of pulsed lidars is not limited by the focusing capabilities of the system but rather by declining Carrier-to-Noise (C/N) ratios at high distances, especially in situations when the number of aerosols in the air is small. In practice, it can reach measurement heights of 40 m up to about 300 m. However, the spatial resolution of pulsed lidar systems is lower than the one of CW lidars and they are much slower regarding the data acquisition. While CW lidars process up to 50 measurement samples per second for commercial systems, pulsed lidars can only handle up to four samples in the same period of time [8, 9].

Several wind lidars addressing the wind energy market are commercially available today. Natural Powers (ZephIR) and OPDI Technologies & DTU Fotonik (WINDAR) produce CW based wind lidars, while Coherent Technologies Inc. (Wind tracer), Leosphere (Wind-Cube) and Sgurr Energy (Galion) manufacture pulsed lidars [8].

1.2.3. Applications for wind energy

A possible and valuable application for wind energy is the replacement of tall reference meteorology (met.) mast installations with lidar measurement systems. Now, the met. mast are required for accredited and bankable wind resource measurements and for ground-based wind turbine performance measurements. Lidar manufactures also offer their wind lidars as instruments for evaluation of model-based wind resource estimation, on and offshore (numerical wind atlases).

Nowadays, wind lidars offer the wind energy industry RS instruments for:

- Wind speed, wind direction, and turbulence profiling;
- Wind resource assessments, on and offshore;
- Wind turbine performance testing (power curves);
- Wind resource assessment via horizontal scanning over complex terrain [8].

1.3. Ship-lidar measurements

1.3.1. Introduction

Since the number of planned wind farm projects has consistently grown during the last years, the relevance of precise wind measurements offshore has increased significantly. Conventional methods such as fixed met masts or lidar devices on fixed platforms have been used until now, but they are connected with high planning effort and costs. A flexible alternative for a various number of application areas is the use of lidar buoy, but in some cases of more particular applications the ship-based lidar system results to be more convenient.

In many cases, ships results to be easy platform where to install lidar systems, especially in the case of service or installation vessels that are located close to the location of interest. Compared to buoy-based solutions, ships offer a more stable platform and can be positioned more easily. Nevertheless, the ship velocity and rotational movements influence the recorded data and therefore need to be considered and corrected. If the quality of the corrected data is adequate, possible applications, besides the wind resource assessment, can be online monitoring during construction processes or short wake and inflow measurements [10].

In order to be able to compute a correction of the measured data with respect to the concurrent motions, an integrated motion measurement system is installed as an essential part of the developed ship-lidar system. Data for the up to six degrees of freedom of the system placed on the ship are recorded with high resolution, processed and applied for a correction of the concurrently recorded lidar data [1].

1.3.2. Fields of application and challenges

One of the main applications for long-term wind resource assessment is the buoy-based system, but also the Ship-Lidar System shows high flexibility. For example, measurements

can be carried out in a tightly focused way and need less time for planning and preparation. This implies a wide range of specific fields of application, such as:

- Short-term measurements for a first evaluation of the wind conditions at a particular site (e.g. during geotechnical screening);
- As assistance for offshore resource assessment campaigns (e.g. for a short-term verification of a lidar-buoy system or numerical modeling);
- Online wind speed reporting during construction phase (e.g. for monitoring of weather windows and verification management);
- Short-term measurement activities during commissioning and operational phase (e.g. rough performance verification or wind farm control optimization).

As a future prospective, all kinds of offshore wind measurements are possible applications of a ship-based measurement system. Furthermore, this kind of application either justifies the specific use of a certain ship or can be carried out alongside a trip that would be done anyway on the route of a given ferry [1].

1.4. Data sources for validation and verification

In order to have a clear idea regarding the potentialities and advantages of a ship-based lidar system, it is necessary to provide an overview of the current methodologies used for the evaluation of wind data sources. Independently of the wind measurement application, which can be, for example, meteorology or wind farm planning, the wind characteristics need to be measured on site. The measurement are then useful for statistical calculations of wind speed distribution and provide the mainly used average values of 10 minutes. In addition to the already described wind lidar (see chapter 1.2.2) observing at hub-height, the main wind data sources are the measurement tower (also called met. mast), the wind lidar buoy, the satellite data, and the data coming from mesoscale weather research and forecasting (WRF) model.

A measurement tower or met. mast is a free standing tower or a removed mast, which carries out not only measurements in order to determine ambient conditions with meteorological instruments such as thermometers and anemometers, but is also used to conduct measurements and analyses on environmental impacts, e.g. upon benthic organisms, fish, bird-, and sea life. Analyses are also intended to facilitate the further development and appraisal of measures, in particular for wind measurements by means of anemometers, which might be implemented for the restriction, or prevention of impacts as the expansion of offshore wind farms proceeds [15].

Figure 1.2 shows an example of met. mast, FINO1, located in the North Sea and used as a reference source for a measurement campaign as explained in Chapter 2.3.1. The meteorological data recorded by FINO1 includes measurements of the wind speed, wind direction, air temperature, atmospheric pressure, atmospheric humidity, and precipitation. The mast can record environmental parameters simultaneously at different heights. In this case, the respective measurement sensors are mounted on a lattice met. mast with a height of 80m which is installed on the platform, and therefore the maximum measuring height is at 103m above the Lowest Astronomical Tide (LAT) [9, 15]. In order to measure the wind speed, the typical instrument used is an anemometer installed at different heights.



Figure 1.2: Offshore met. mast FINO1 in the North Sea at the location N54 00' 53,5" E 6 35' 15,5". FINO1 measures among other things the wind speed, wind direction, air temperature, atmospheric pressure, atmospheric humidity and precipitation. The wind speed is retrieved at 100 m height and further lower heights [15].

Wind lidars are a relative new technology used in the field of wind measurements. As explained in Chapter 1.2.2, lidars use light beams and the Doppler effect to detect a small frequency shift in the very weak backscattered light resulting from the many small aerosols suspended and moving with the air aloft. Main applications of lidars are ground-based systems used as wind “profiler”. A wind profiler measures 10-min averaged quantities of the vertical wind speed profile, the vertical direction profile, and the vertical turbulence profiles, by combining a series of radial wind speed components measured using several, and at least three, different beam directions, into a three-dimensional wind vector. CW-based wind lidars, e.g. the ZephIR, can measure the vertical wind profile from 10 m to 250 m height at ten consecutive heights selectable in this range. Pulsed lidars, e.g. the Wind-Cube or the Galion,

measure correspondingly the vertical wind profile in the height range from 40– to approximately 300 m simultaneously at several (of the order of 10) heights. In the case of pulsed lidars, the upper bound depending on the amount of aerosols in the air [8]. Wind lidars can also be used in experimental systems that can be mounted on the nacelle of a wind turbine or integrated into the rotating spinner to measure oncoming horizontal winds, winds in the wake of the wind turbine, and proactively adjust blades to protect components and increase power. In this case, it is possible to talk about wind profiling lidar observing at hub-height.

Lidar buoy is a further alternative to conventional met masts: first, it is much more flexible since it is kept at its position by an anchor chain that allows the buoy to be moved easily to another location. Furthermore, the permissions for locating the buoy in the sea can be achieved much faster than permissions for construction of a met mast, the installation allows a big saving in price (5 to 10 times cheaper) and requires an easier maintenance compared to a met mast. As a lidar technology, the measurement height on a buoy can reach more than 200m and can measure wind speed in a selectable range.

On the other hand, the lidar buoy is much more subject to the rough offshore conditions than the measurement devices on a met mast. First, the lidar needs to be adapted to a common marine buoy and protected from salt and water. In case of the lidar buoy implemented by Fraunhofer IWES, this is done through an aluminum box with special glass at the top so that the light beams are not distorted [2]. In addition, since the buoy is rotating, the influence of the waves on the measurements needs to be removed and therefore a motion correction algorithm is necessary.



Figure 1.3: Fraunhofer IWES wind lidar buoy [2]. The lidar is adapted to a common marine buoy and protected from salt and water through an aluminum box with special glass at the top so that the light beams are not distorted.

Other than wind lidar, observations from satellites are a kind of technology that can provide wind data at a relatively low cost. Satellite remote sensing is based on measurement techniques using Earth observation (EO) space-borne instruments such as thermal infrared radiometers to obtain the sea surface temperatures and optical visible and near-infrared bands on various instruments that provide ocean parameters such as chlorophyll and turbidity. In order to obtain wind velocity, microwave remote sensing can be useful since it has the advantage of penetrating clouds and thus observations are available during rainy or cloudy conditions as well [12].

The microwave observations can be passive or active (radar) and the main types are represented in Figure 1.4. The approximate spatial and temporal scales and dominant application domains are indicated. Passive microwave observations have the longest archive starting in 1987 and with up to six observations each day with near-global coverage using a suite of satellites. Scatterometers have around the same spatial resolution and a global coverage of approximately twice a day. On one hand, scatterometer data provide wind vectors whereas passive microwave data provide wind speed only. On the other hand, the two

remaining types of microwave instruments, altimeter and synthetic aperture radar (SAR), have been designed for other purposes but their measurements can be used to study wind field over the sea surface as well. An altimeter provides wind speed whereas SAR provides wind vectors by combining wind direction information from e.g., SAR directional analysis, sea surface Doppler shift, or using input from an atmospheric model to the wind product. The advantages of SAR are the very high resolution, which can reach 400 m for current wind field products, and the fact that coastal regions are covered as well. The availability of the data results to be lower compared to other sources because both the archives of altimeter and SAR data sets are sparser in space and time [12].

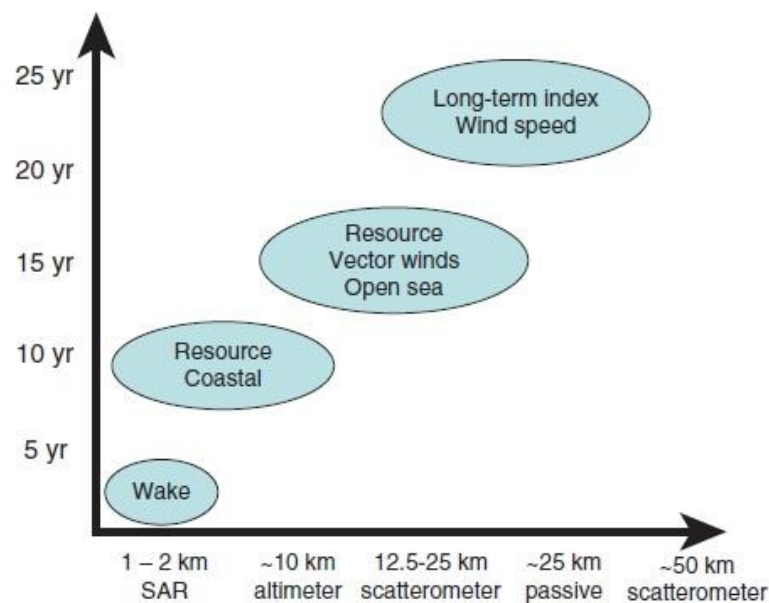


Figure 1.4: The diagram shows the main ocean wind satellite technology types, their spatial and temporal resolutions, and their main application domains [12]. The x-axis represents the spatial resolution where the SAR highest resolution that can reach up to 400 m; the y-axis corresponds to the temporal resolution that depends on the type of satellite and on the kind of application.

In sum, the advantages of microwave satellite remote sensing are:

- horizontal spatial coverage,
- long data archives,
- high spatial detail, both in the coastal zone and offshore wind farm wake.

A drawback of this technology is that winds are observed at 10m above sea level and therefore there is the need to extrapolate in the vertical direction to hub-height i.e., vertical extrapolation.

Finally, a brief description of the WRF data is provided. The WRF model is a mesoscale numerical weather prediction system designed in the 1990s for both atmospheric research and operational forecasting needs. It has been developed in the United States thanks to a collaboration among the National Center for Atmospheric Research (NCAR), the National Oceanic and Atmospheric Administration (represented by the National Centers for Environmental Prediction (NCEP) and the (then) Forecast Systems Laboratory (FSL)), the Air Force Weather Agency (AFWA), the Naval Research Laboratory, the University of Oklahoma, and the Federal Aviation Administration (FAA). The model serves a wide range of meteorological applications across scales from tens of meters to thousands of kilometers and one of these applications is of course the retrieval of wind data [13].

On one hand, similar to satellite data, the WRF data have a high spatial coverage and can provide different resolutions. On the other hand, the temporal resolution of the WRF data is finer since these data can provide up to 30-min average value of wind speed, while the temporal resolution of the satellite data is limited to the effective availability. Both the spatial and temporal resolutions depend on the input data and the CPU time. On one hand, this mesoscale model is widely used all over the world for weather forecast and therefore is a valid source for the validation of wind data sources. On the other hand, also the wind data sources can be useful to validate the WRF models.

The following table summarizes the above described wind data sources and compares them in order to highlight advantages and drawbacks of each source compared to the others.

	Lidar	Lidar Buoy	Satellite	WRF
<i>Met. Mast</i>	<p>Both sources do not need motion correction</p> <p>Both anemometer and lidar have good measurement agreement</p> <p>Lidar can measure at higher heights</p> <p>Met. mast is a well-known system while lidar is a new one, although with good quality data</p> <p>Linear regression coefficients between lidars and cup anemometers: range of $\sim 0.99-1.00$ [8]</p>	<p>Lidar needs correction for the rotation</p> <p>As a lidar, it provides measurements at higher heights</p> <p>Lidar buoy: more flexible, lower installation and maintenance cost, fewer permissions required for installation</p> <p>Met. mast less subject to rough offshore conditions</p>	<p>Met. mast gives a punctual information, while satellite data regard an area</p> <p>Met. mast provides a time series with very high temporal resolution, while the revisit times of the satellite data are less frequent, possibly sparse, and mission-dependent</p>	<p>Met. mast gives a dense time series but a punctual information in space, while the WRF provides an instantaneous information every 30 minutes and over an area</p>
<i>Lidar</i>		Fixed lidar does not need motion correction	Lidar gives a dense time series of punctual information, while satellite gives area-based less frequent data	Lidar gives a punctual information over time, while WRF instantaneous data every 30 min over an area
<i>Lidar Buoy</i>			See fixed lidar	See lidar buoy
<i>Satellite</i>				The satellite provides data only twice a day (at most), while WRF gives data every 30 minutes (also 10-min is possible)

Table 1.1: Comparison among different wind data sources.

2. CHAPTER II: METHODOLOGY

2.1. Ship-lidar data as an offshore wind resource assessment

Offshore lidar devices can be installed on fixed platforms, on buoys, or on ships. Together with a number of commercial product developments, the number of buoys installed has significantly increased in the past years because of several advantages in comparison with met. mast, as explained in chapter 1.4. Depending on the type of application, an anchored buoy can be either more or less convenient when compared to a ship-based lidar system.

For long-term applications, not only measurements from fixed platforms or anchored buoys are a recommendable solution, but also ship-based solutions are, in particular when applied on regular ferry routes. Moreover, since there are still a number of scenarios where the flexibility of buoy-based systems does not match the needs, e.g. if the location has to be changed often, and if a vessel in proximity to the location of interest is available, this one can be used as a platform for the measurement device [14]. Thus, an evident advantage of this new technology is the possibility to install the system on an already existent ferry route that corresponds to the location of interest.

In comparison with buoy-based solutions, ships offer a more stable platform and can be positioned and installed easily. Nevertheless, influences from the ship velocity and rotational movements have to be considered and corrected. If the quality of the corrected data is adequate, applications can be online monitoring during construction processes or short wake and inflow measurements [10].

One of the main objectives of this work is to evaluate the applicability of this new measurement system and the reliability of the possible correction methods. Therefore, in the next chapters an overview of the projects and measurement campaigns and the methodologies used for the corrections are explained.

2.1.1. Projects and measurement campaigns

Two different ship-lidar measurement campaigns are taken into account in this thesis in order to evaluate the ship-lidar data: one in proximity of the Alpha Ventus wind farm and FINO1 as a part of the European Energy Research Alliance - Design Tool for Offshore Wind Farm Cluster (EERA-DTOC) project, and the other one in the ship's route from Bremerhaven to Helgoland.

The first one has been performed from 10 to 15 June 2014. The main goal was the detection of wind turbine and wind farm wakes, but also the verification of the ship-lidar measurement as well as different motion corrections. Therefore, measurements under typical motion influences in proximity to FINO1 were executed [16].

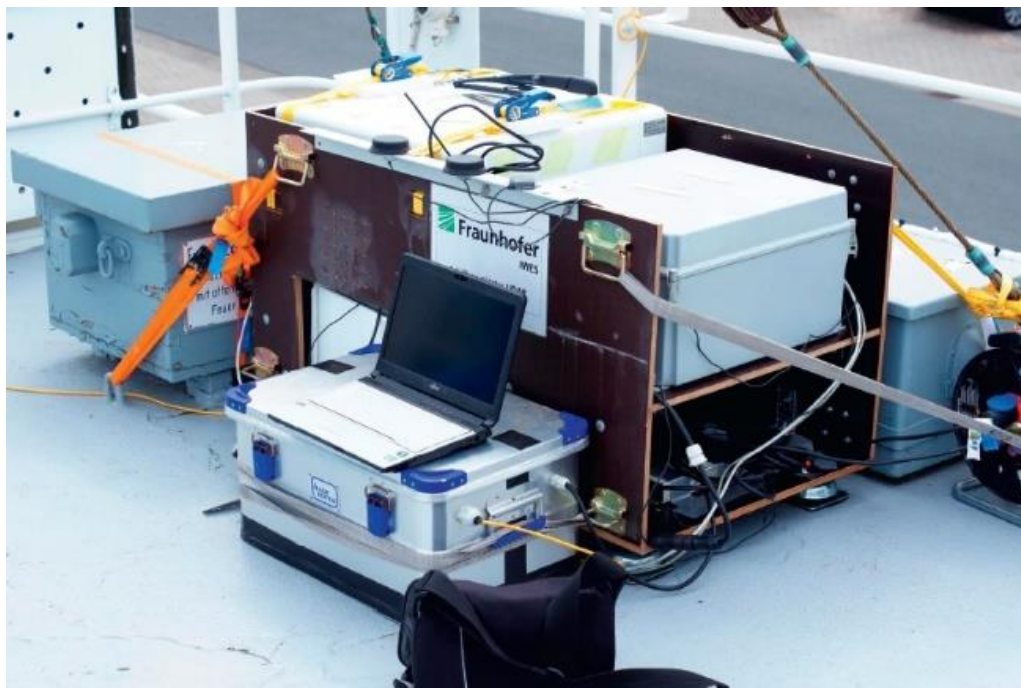


Figure 2.1: Lidar and sensor box installed in the frame, fixed to the top deck of the LEV Taifun [14]. The ship-lidar system used for the wake measurements includes a lidar, which is a Leosphere Windcube V2 Offshore edition, together with motion sensors, communication devices, and a ruggedized computer.

Figure 2.1 shows the lidar sensor installed in the frame for the measurements and the offshore support vessel LEV Taifun used for the campaign. The ship-lidar system used for the wake measurements comprises a lidar, motion sensors, communication devices, and a ruggedized

computer. The main component is a Leosphere Windcube V2 Offshore edition. The lidar performs a velocity-azimuth display (VAD) scanning pattern including a fifth vertical beam. A combination of an xSens MTi-G attitude and heading reference sensor (AHRS) and a Trimble SPS361 satellite compass is needed in order to obtain motion information that will be useful for the correction of the lidar data. The MTi-G sensor has a static accuracy better than 0.5° and is used with a sampling frequency of approx. 10 Hz. The satellite compass has a heading precision of under 0.1° for the configuration used here [14].



Figure 2.2: LEV Taifun during measurement campaign in proximity to FINO1 [16]. The ship navigated in proximity of the FINO1 met. mast in order to use it as a reference for the comparison.

Figure 2.2 shows the lidar sensor installed on the offshore support vessel LEV Taifun used for the campaign in proximity to FINO1. During this campaign, the met. mast FINO1 has been the reference source of wind speed data in order to compare and evaluate the data coming from the ship-based lidar and the information provided by the satellite compass allow to apply the motion correction method.

The second measurement campaign evaluated in this thesis has been performed from 02 June to 22 August 16 on the MS Fair Lady ship. The data have been registered continuously even

when the ship was moored in the harbors of Bremerhaven and of the island of Helgoland. Figure 2.3 shows a map of the area of interest and highlights the two main ports.

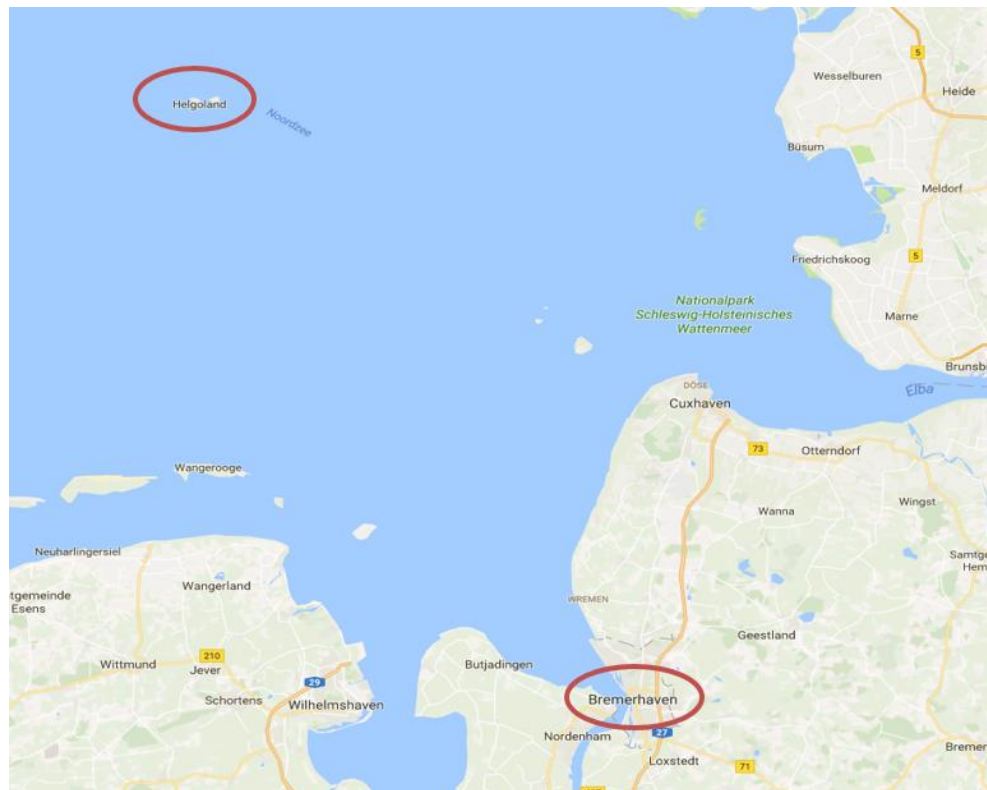


Figure 2.3: Map showing the start and end locations of the ship route in the two red circles - ©2017 GeoBasis-DE/BKG (©2009).Google

The wind data obtained during this campaign have been processed and corrected as explained in the following chapters. In order to validate this correction method, the data have been compared with data from the German Weather Service (DWD) and the mesoscale simulation data coming from the WRF model.

2.2. Ship-lidar system

2.2.1. Measurement principle

The data registered by the WindCube and used during this work were processed directly by the lidar applying the following approach. The WindCube measures at four azimuth angles, e.g. north, east, south and east. In this case, the coordinate system is such that u is aligned in the mean wind direction.

$$u = u_{NS}\cos\theta + u_{EW}\sin\theta \quad (2.1)$$

$$v = u_{NS}\sin\theta - u_{EW}\cos\theta \quad (2.2)$$

where u_{NS} and u_{EW} denote wind speeds in the north–south and east–west directions, respectively, and θ denotes the wind direction [22].

From simple geometrical considerations (see Fig. 2.4),

$$u_{NS} = \frac{\tilde{v}_{rN} - \tilde{v}_{rS}}{2\sin\Phi} \quad (2.3)$$

$$u_{EW} = \frac{\tilde{v}_{rE} - \tilde{v}_{rW}}{2\sin\Phi} \quad (2.4)$$

where \tilde{v}_{rN} , \tilde{v}_{rS} , \tilde{v}_{rE} , and \tilde{v}_{rW} are the weighted average radial velocities in the north, south, east, and west directions, respectively, and Φ is the half-opening angle of the laser beam. For the w component in Fig. 2.4,

$$w_{WC} = \frac{P(\tilde{v}_{rN} + \tilde{v}_{rS}) + Q(\tilde{v}_{rE} - \tilde{v}_{rW})}{2\sin\Phi} \quad (2.5)$$

where P and Q are the weights associated with the wind direction such that $P + Q = 1$ and $P = \cos^2\theta$ and $Q = \sin^2\theta$ [22].

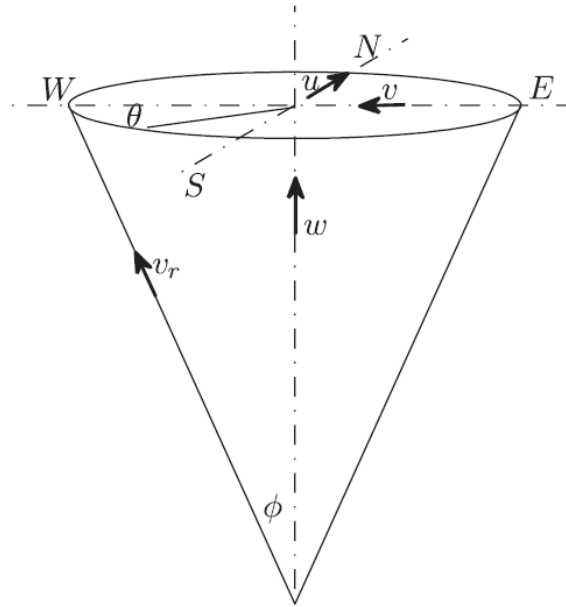


Figure 2.4: Schematic of the velocity–azimuth display scanning [22].

By plugging Eqs. (2.3) and (2.4) into Eq. (2.1) it is possible to obtain the searched wind vector, but of course the motion influence of the ship need to be taken into account.

2.2.2. Motion influence on ship-based lidar measurements

In order to obtain a precise measurement from a moving ship, the correction of the measured data with respect to the concurrent motions is needed. Hence, an integrated motion measurement system is an essential part of the developed ship-lidar system. The satellite compass that provides also yaw/heading and information about velocity (course over ground, speed over ground) gives the positioning data.

The data of the system placed on the ship are recorded with high resolution, processed, and applied for a correction of the concurrently recorded lidar data. The processing and the correction are necessary to obtain usable wind data, since recorded data are influenced by the translational and rotational motions of the lidar system.

Rotations of the system change the effective line-of-sight orientation, and thus the projection of the wind velocity on the laser beam as well as the measurement volume. Results of past theoretical and experimental studies show that the 10-min mean wind speed is only slightly influenced by rotational motions if the mean tilting angle of the system is around zero degree

[11]. If a ship experiences strong roll motions, triggered by waves exciting the ship perpendicular to the ship-centre line. In particular under courses perpendicular to the wind direction or under a transposition manoeuvre, roll motion and thus increased virtual turbulence intensity occur.

The yaw motion gives another influence, which is caused by the turning rotation of a vessel about its vertical/Z axis. An offset or deviation is corrected by means of the Trimble data provided by the Global Positioning System (GPS).

Translations generate an additional obtained velocity component along the line of sight (LoS) and its effect depends on the time scale of the motion. Short-term motions only interfere with a small number of line of sight measurements leading to artefacts in the solution during the recalculation of the wind vector. In case of long-term movements that are constant for the time interval covered by the linear system of equation, the measured vector is a result of the vector interference of wind velocity and system velocity.

Therefore, the resulting effects on the distorted measurement data have to be corrected using a motion correction. In order to correct motion-affected wind-lidar data, two different methods can be applied as showed in Figure 2.5: complete motion correction and simplified motion correction [11].

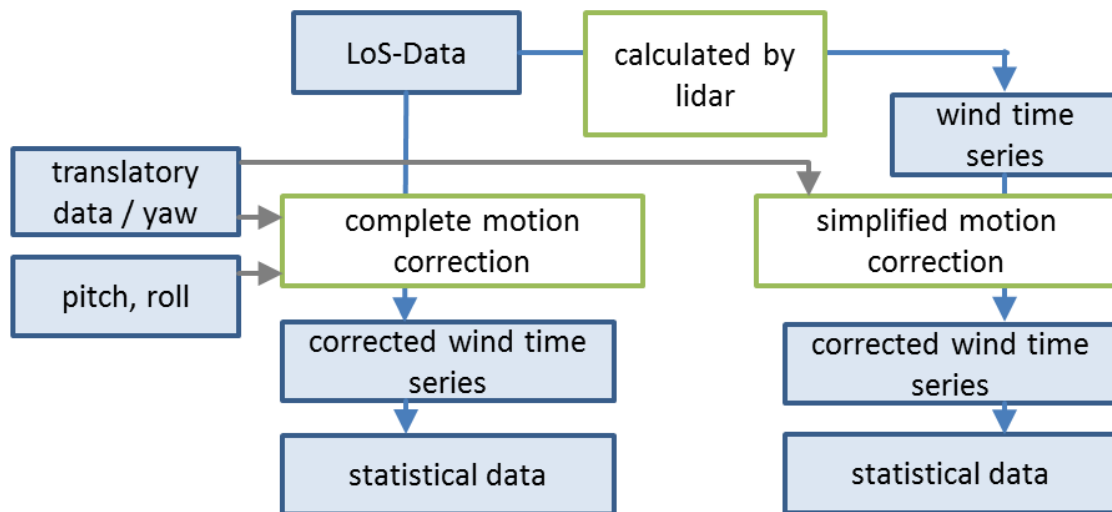


Figure 2.5: Data flow of the different correction algorithms [11].

For a first data analysis and testing of the motion data, a simplified ship correction method can give a first impression of the measured data. This simplified correction takes into account only translatory ship motions and yaw information and uses them on the vector-valued wind time series calculated by the lidar system. The resulting output parameters are the 10-min mean wind speed and direction, calculated every minute using a moving average. Furthermore, a position parameter describes the position of the ship for every time instant. The detailed methods are explained in the following paragraphs but are not applied for the thesis work.

2.2.3. Complete motion correction

The tilted beam orientations are taken into account in a matrix denoted as O_{tilt} . In this way, the tilting motions in the linear system of equations for fixed lidar systems is considered. Furthermore, translatory system motions v_{sys} are considered, resulting in

$$O_{tilt} \cdot u = v_{wind} + v_{sys} \quad (2.6)$$

Additionally changes in the height of the measurement volumes are considered by an interpolation. This formulation, combined with the linear system of equations (LSE), is considered as the complete motion correction.

For the implementation of this correction algorithm, the orientations of all used sensors with respect to each other have to be known. Furthermore, the time lag between the different sensors has to be determined, in particular for short-term motions like roll and pitch. Due to the periodic nature of tilting, heave and surge motions, finding the correct values is complex. The determination of these values is referred to as the calibration of the algorithm.

As a result, the implementation of the motion correction is costly in terms of time for calibration of the algorithm as well as of processing time of the correction algorithm itself. Furthermore, data gaps in only one of the used sensors lead to data loss in the overall corrected wind velocity data.

2.2.4. Simplified motion correction

If the time scales of motion and orientation changes are much longer than the reference time scale, the motion influences are approximately constant for the whole system, and the correction is applied after calculating the wind vector u . Hence, we get

$$u = R_{yaw,pitch,roll} \cdot u_{measured} - u_{system} \quad (2.7)$$

where $u_{measured}$ is the solution of the LSE, $R_{yaw,pitch,roll}$ is the rotation matrix for one point in time, and u_{system} is the ship velocity vector [11]. Furthermore the equation is simplified under the assumption of a quite stable platform without dynamic tilting and static tilting angles to

$$u = R_{yaw} \cdot u_{measured} - u_{system} \quad (2.8)$$

Eventually, the corrected value of wind speed is obtained. From the velocity components, it is possible to retrieve the wind direction value. This is done with the four-quadrant inverse tangent algorithm in the corresponding implementation in Matlab®, which is the software used for the whole processing of the data. The algorithm returns values in the closed interval $[-180^\circ, 180^\circ]$.

This simplified correction is a method that gives the opportunity to implement quickly the motion correction, especially if tilting data are corrupted. In addition, this can be used as a first validation of lidar and motion data before applying the complete motion correction but, in this case, the initial assumption, like slow changes in the motion and low tilting angles, need to be fulfilled.

After the simplified correction has been applied, the last step of the lidar data processing consists of applying the 10-min average, the standard timestamp used for wind data. The average chosen for the processing is the moving average, a calculation to analyze data points

by creating series of averages of different subsets of the full data set. This process is commonly used with time series data to smooth out short-term fluctuations and highlight longer-term trends or cycles.

Given a series of numbers and a fixed subset size, the first element of the moving average is obtained by taking the average of the initial fixed subset of the number series. Then the subset is modified by "shifting forward" the window used for averaging, that is, the first number of the series is removed from the subset and the next number following the original subset in the series is added to the subset itself. This creates a new subset of numbers, which is averaged [17]. This process is done in order to obtain a 10-min average value and is shifted every minute forward; then, the process is repeated over the entire data series and thus the final dataset contains more data points, compared to a simple average, that can be chosen and used for further comparisons.

2.3. Ship-lidar verification and comparison

The processing of the lidar data is fundamental in order to proceed with their verification and comparison with other sources. In particular, since there is the need to obtain a precise measurement from a moving ship, the correction is essential otherwise the data would not be usable.

This can be done thanks to the integrated motion measurement system and the simplified motion correction. The resulting wind speed and direction values are averaged with a 10-min moving average that is shifting every minute and, depending on the other source the data need to be compared with, one can use either the whole dataset or only the data needed. Besides the suitable averaging processing, also the information coming from the satellite compass is a prerequisite for the comparison with those kinds of wind data sources that have information both in time and in space.

One of the comparison that have been carried out is between the lidar and FINO1 data recorded during the campaign of June 2014 as part of the EERA-DTOC project. A previous detailed analysis of the lidar data and motion correction was already done as described in [16] and therefore this study can be a further validation of the simplified motion correction method.

Another possibility to check the processed lidar data with an available data source is the comparison between lidar and the DWD source. This step has been done with the dataset from the Helgoland campaign and it results to be useful even if for this kind of route the level of comparison is limited since the DWD provides only one-hour mean data.

The same dataset has been compared daily and monthly with the WRF data. This allows checking if the ship-based lidar source can be valid for wind resource assessment and potentially substituting a met. mast or not. Furthermore, a critical point is checking whether the use of the ship as a lidar platform can be useful to validate WRF models when focused on specific campaigns or not.

In the same way and using a similar procedure, the lidar data can be compared with satellite data. This can be of particular interest when looking at wakes and can be part of future research work.

2.3.1. FINO1 campaign: FINO1-Lidar comparison

Main goal of this paragraph is the verification of the ship-lidar measurement itself. Therefore, within the FINO1 campaign, measurements under typical motion influences in proximity to FINO1 have been executed and afterward corrected. The measurement campaign, as well as the comparison, are described.

The FINO1 research platform is located 45 km north-west of the Borkum island in the North Sea at the location N 54 00' 53.5" E 6 35' 15.5" and has been in operation since Autumn 2003. The German Federal Ministry for the Environment, Nature Conservation, Building, and Nuclear Safety funded it in order to investigate several environmental parameters relevant for the construction of offshore wind farms in the German North Sea [FINO1 reference, 9].

In close proximity east of FINO1, the first wind turbines of the offshore wind farm Alpha Ventus started operation in August 2009 [9]. Moreover, both the Trianel Windpark Borkum wind farm located in the northwest of FINO1 and the Borkum Riffgrund I wind farm, which is situated in the southwest of FINO1, started to operate in the beginning of 2015 [9, 18]. The location of FINO1 and the wind parks is shown in Figure 2.6.

As well as for the other campaigns, the measurement from the FINO1 campaign have to be processed and corrected as explained in chapter 2.2.4. The data available from the measurements and used for the comparison were collected from 11 to 14 June 2014. Figure 2.7 shows the track of the ship in proximity to FINO1 and the Alpha Ventus wind farm.

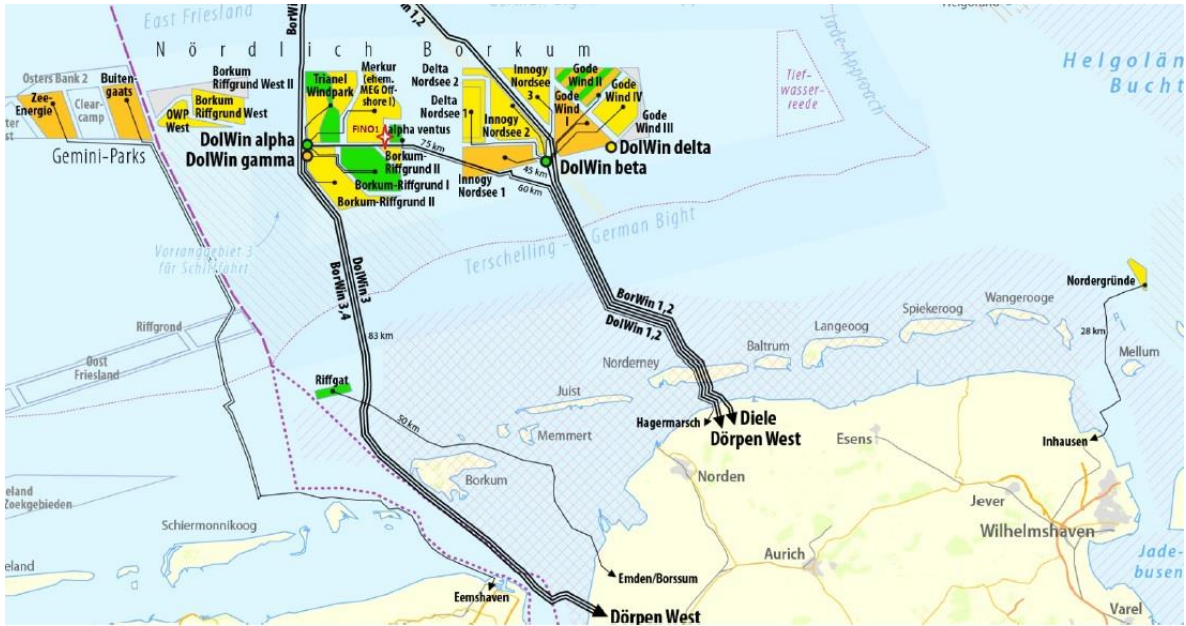


Figure 2.6: Extract of map showing offshore wind parks in the German Bight with the location of FINO1 marked red. Green: wind farms and converters in operation, green/orange: partial commissioning, orange: under construction, yellow: approved, gray: requested [9, 18].

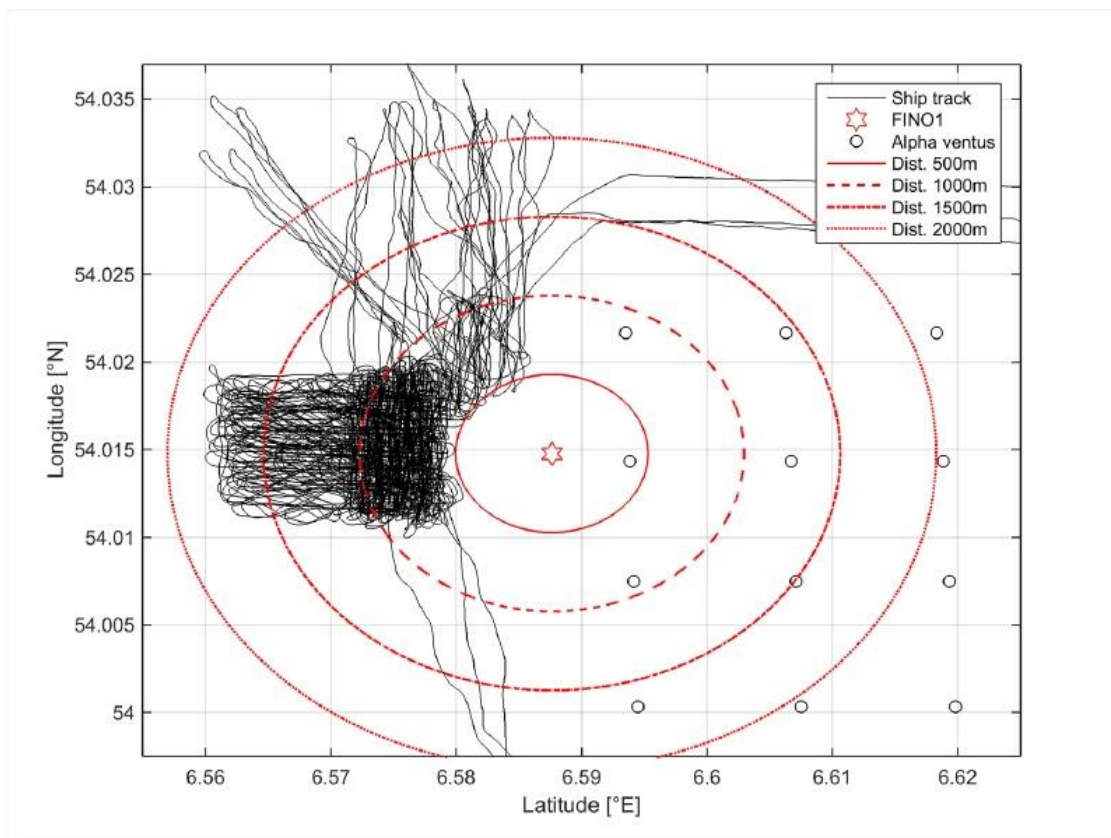


Figure 2.7: Ship track in proximity to FINO1 [16].

For assessing data accuracy, the following filters, based on the reference data from FINO1, are applied. In particular, for the assessment of wind speed accuracy:

- Distance between ship and reference < 2 km
- Reference wind direction values with pre-defined valid wind direction sector (see below).

In order to define the valid wind direction, both mast and site characteristics and their influences on the measurements need to be considered in detail. For this purpose, Figures 2.8 and 2.9 show the relative deviation between the wind speed measurements of the lidar system and the reference cup anemometers versus the reference wind direction for two different heights. Obvious systematic deviations due to the effects of the mast and the wind farm have to be filtered out by applying a suitable wind-direction filter [11].

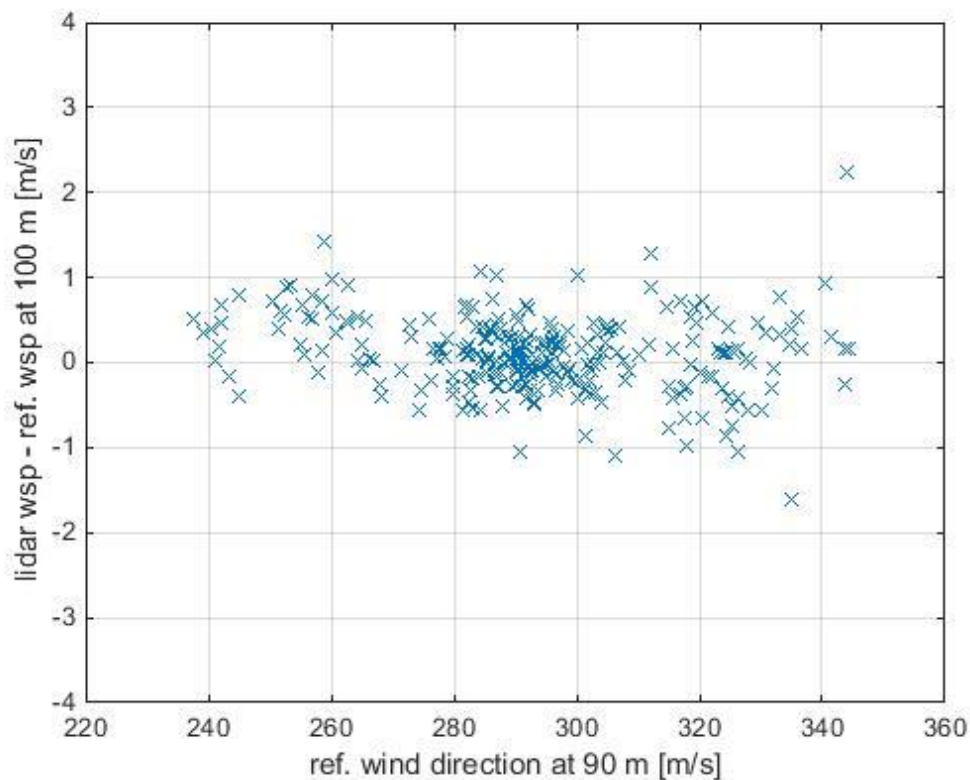


Figure 2.8: Wind speed deviation (lidar – FINO1) at 100 m versus wind direction at 90 m.

The height of the lidar was approx. 7 m over the sea level, therefore this additional altitude had to be taken into account while considering the lidar data. The resulting valid wind direction sector for the assessment of wind speed accuracy at 100 m is $(230 - 330)^\circ$. The points considered are below 2 km distance from FINO1 for a total of 271 data points.

Note that there is no reference wind direction measurement at 100 m. That is why the vane measurements at 90 m are used instead.

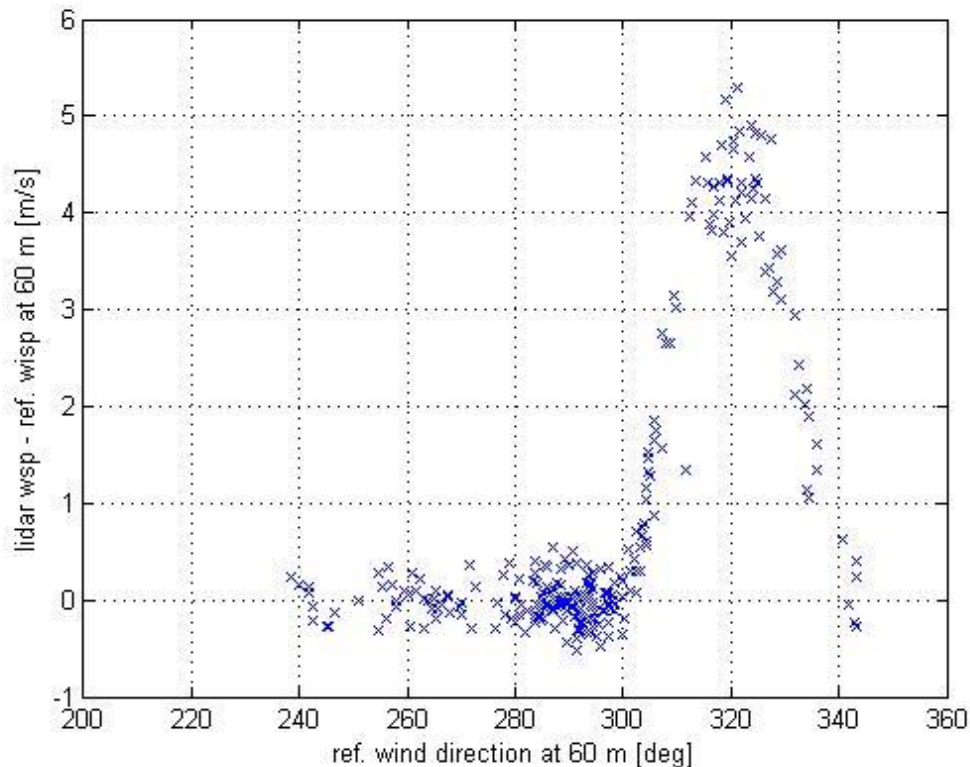


Figure 2.9: Wind speed deviation (lidar – FINO1) versus reference wind direction at 60 m.

As it is possible to see from Figure 2.8, the plot shows a better correlation for points with wind direction lower than 300 degrees. The resulting valid wind direction sector for the assessment of wind speed accuracy at 60 m is $(230 - 290)^\circ$. The number of points considered below 2 km distance from FINO1 is 271 as well as the previous case since the days considered are the same.

2.3.2. Helgoland campaign: DWD-Lidar comparison

The comparison between lidar data from the Helgoland campaign and the DWD source is a first step of validation after the lidar data have been processed. The German Weather Service can be easily accessed through an online database in order to retrieve weather information and provides a wide range of services. Thus, the data regarding the period of interest and located in Bremerhaven and Helgoland harbors are obtained from the online source [19].

Figures 2.10 and 2.11 show the location of the met. mast in the two main ports with respect to the position of the ship. The distance between these two is approximately 1.14 km when the ship is in the port of Bremerhaven and less than 500 m when it is in the port of Helgoland. Therefore, the influence of these distances, which are variable depending on the day, can be negligible when comparing the two datasets.

These are the geographical coordinates of the met. masts:

- Bremerhaven met. mast coordinates: 53.5332, 8.5761
- Helgoland met. mast coordinates: 54.175, 7.892.

The wind speed is obtained from lidar measurements at a height of 50 m, while the met. masts in Bremerhaven and Helgoland have a sensor height above ground of 11.6 m and 10 m, respectively. This might be a first reason of a larger deviation because of the different measurement heights. Furthermore, since the DWD database provides only hourly means of wind speed and direction of the climatological time series, the 10-min average values coming from the lidar measurement and considered for the comparison are a simple average. The time series has only been plotted and graphically compared and no further procedure has been applied to the lidar data. Based on these considerations, this step of the work is a preliminary validation.



Figure 2.10: The port of Bremerhaven with the position of the ferry and the met. mast. The distance between these two is approximately 1.14 km and therefore it can be negligible when comparing the data - ©2017 Aerowest, DigitalGlobe, GeoBasis-DE/BKG, GeoContent, VuK BHV, GeoBasis-DE/BKG (©2009). Google.



Figure 2.11: The port of Helgoland with the position of the ferry and the met. mast. - ©2017 DigitalGlobe, GeoBasis-DE/BKG, GeoContent, Landsat, GeoBasis-DE/BKG (©2009). Google.

2.3.3. Helgoland campaign: WRF-Lidar comparison

The comparison between lidar and WRF data allows not only to better check if the lidar data are usable for wind resource assessment, substituting the conventional met mast with considerable advantages, but also as a first basis to evaluate if this wind data source can be useful to validate the WRF models. Measurements need less time for planning and preparation and give good results in specific fields of application such as: short-term measurements either for a first evaluation of the wind conditions at a particular site or for commissioning and operational phase, as assistance for offshore resource assessment campaigns and also for monitoring of weather windows and verification management.

WRF works with a staggered Arakawa C-grid that is showed in figure 2.12. This means that the simulation results are not available at the same position in the grid for all variables. Components of the wind velocity vector are U, V, W but on flat ground, W on the first discretization level is zero. However, when the ground has nonzero slope, the vertical velocity components W is generally not zero, because the normal vector to the ground is not vertical.

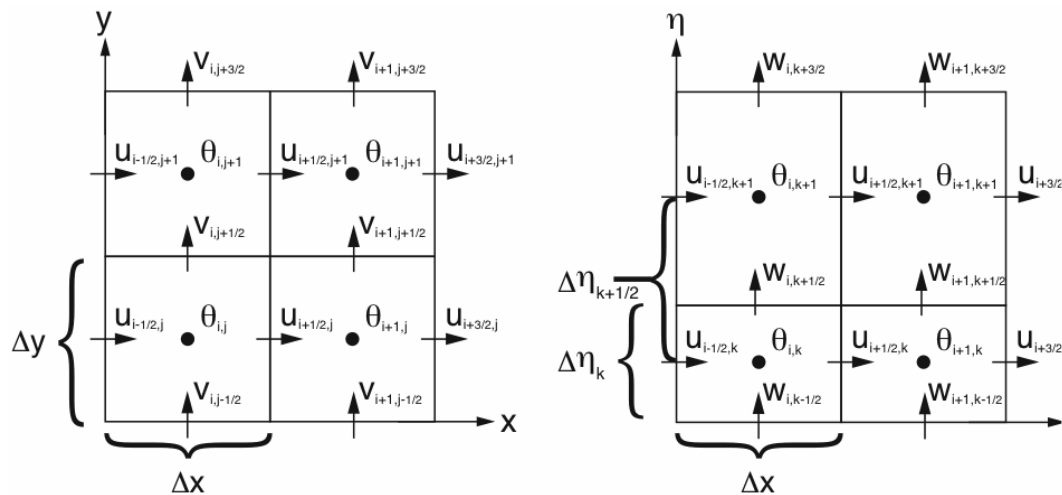


Figure 2.12: Arakawa grid of WRF models. The left grid shows the axis on the horizontal plane that are all equally distributed, while the right grid shows how the cells change in the vertical direction [20].

The U- and V - component of the wind are defined on different positions of a cell and therefore the data are interpolated to a common position θ in the centre of the cell in order to be processed. XLAT and XLONG describe the positions of the mid points θ projected to the horizontal plane. Therefore, the picture 2.12 uses half integer indexing. In order to proceed with the analysis, U and V are interpolated to θ in such a way that the numbers of their values in the i- and j-directions become the same, which is a benefit for further investigation [2, 20].

The wind components are stored in the following way:

- The horizontal wind component $U_{i-1/2,j,k}$ in the X direction in the array entry $u(i, j, k)$;
- The horizontal wind component $V_{i,j-1/2,k}$ in the Y direction in the array entry $v(i, j, k)$;
- The vertical wind component $W_{i,j,k-1/2}$ in the array entry $w(i, j, k)$.

In particular, the lowest layer in WRF is indexed with $k = 1$, and, on flat ground, $w(:, :, 1) = 0$, since the ground is impermeable in the normal direction. On a ground with nonzero slope, $w(:, :, 1)$ is generally nonzero. The winds at the middle of the first layer, at the height η_1 , are $u(:, :, 1)$, $v(:, :, 1)$ and they are generally nonzero [20].

Because the components of the wind velocity vector are on different staggered grids, and visualization software usually expects all three components of the velocity vector based at the same point, they need to be interpolated to θ -points (cell centers) for display:

$$\begin{aligned}
 U_{\theta}(i, j, k) &= 0.5 * (U(i, j, k) + U(i + 1, j, k)) \\
 V_{\theta}(i, j, k) &= 0.5 * (V(i, j, k) + V(i, j + 1, k)) \\
 W_{\theta}(i, j, k) &= 0.5 * (W(i, j, k) + W(i, j, k + 1))
 \end{aligned}
 \tag{2.9}$$

The same applies for the vertical axis. Values of PHB and PH, whose sum is the geopotential, are defined on the pressure levels η_k and horizontally in the middle of the cell like the terrain height HGT. So they need to be interpolated to θ as well. The hydrostatic pressure variable η is not equally distributed in the vertical direction so the height of each cell is different at each level and point in time.

After the interpolation in the horizontal plane has been made, the right cell in the vertical direction containing the measurement height needs to be found. The simulation results are given in pressure levels which change with time and therefore the vertical index k_0 of the cell may vary each time step as showed in Figure 2.13. Thus, the cell needs to be detected every time step to interpolate the right variable values to the desired height. With given perturbation geopotential PH $[m^2/s^2]$, base-state geopotential PHB $[m^2/s^2]$, and terrain height HGT [m] simulated with WRF, the heights of the top and bottom of the cells above the surface can be calculated with:

$$z = \frac{PH + PHB}{9.81 \text{ m/s}^2} - HGT \quad (2.10)$$

The distribution of the levels in height are so dense that linear interpolation can be applied to get the height of the centre of the cells and the variable values [20]. Figure 2.13 shows how the pressure levels can vary in space and time.

$$z_\theta = \frac{PH(i, j, k) + PHB(i, j, k) + PH(i, j, k + 1) + PHB(i, j, k + 1)}{9.81 \text{ m/s}^2} - HGT \quad (2.11)$$

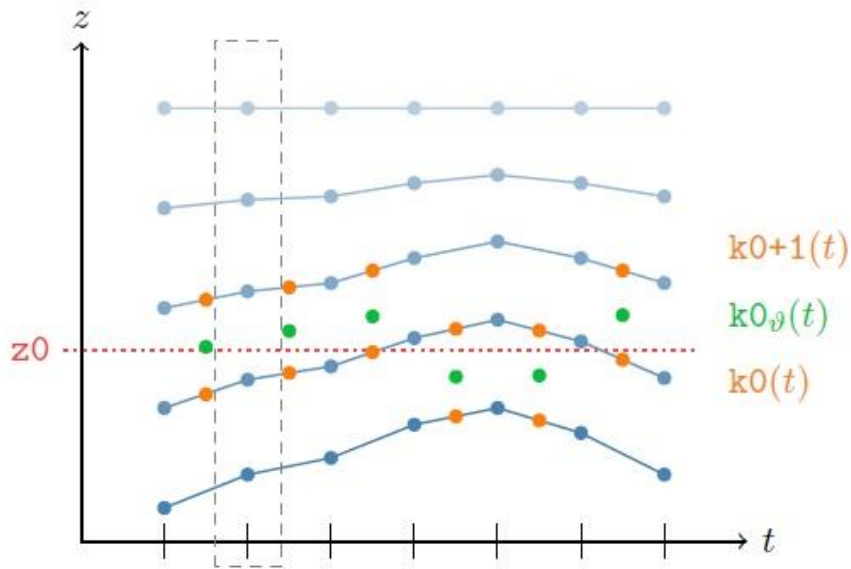


Figure 2.13: Interpolation from pressure levels η to measurement height z_0 [2].

The projection of the earth surface would need to be considered and requires a certain correction, which has been neglected for this calculation. Hence, once the U_z and V_z components have been calculated, the horizontal wind speed is obtained from:

$$U_{hor} = \sqrt{U_z^2 + V_z^2} \quad (2.12)$$

Based on these considerations on the WRF model, it is possible to explain the procedure used to analyse the WRF data in order to compare them with the lidar source.

Figure 2.14 shows the route of the ship from Bremerhaven to Helgoland and the way back. The way to the island and back is supposed to be every day the same, except possible deviations as shown in the pictures below.

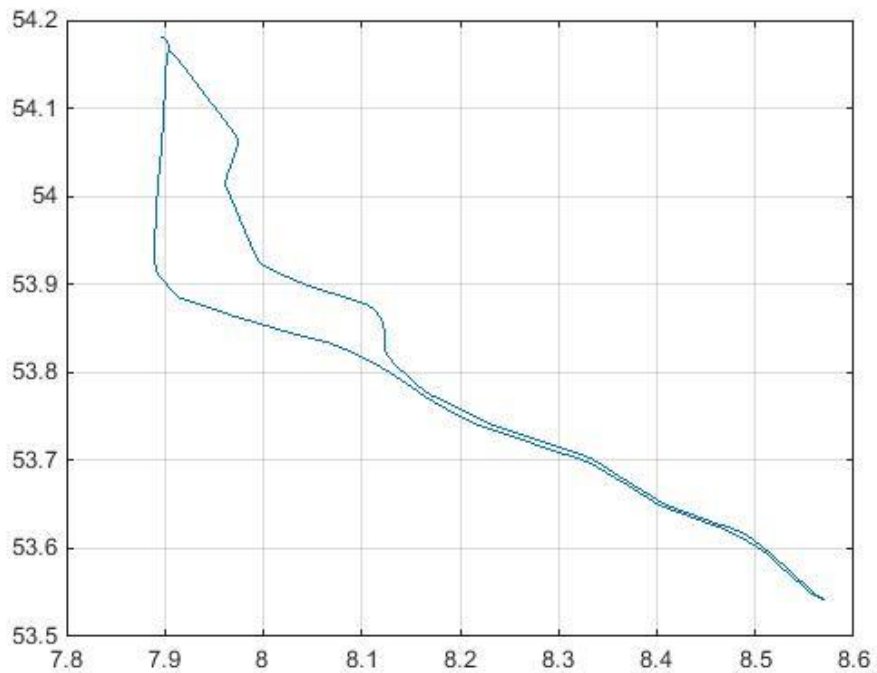


Figure 2.14: Route of the ship from Bremerhaven to Helgoland and way back. The positioning data are retrieved thanks to the satellite compass and plotted with Matlab®.

Figure 2.15 shows the route of the ship from Bremerhaven to Helgoland and the way back on the 3 of July 2016 obtained from the Matlab® routine. This uses the coordinates of the ship taken from the satellite compass ($N = 86400$ seconds per day) and finds the closest point in the Arakawa-grid of the WRF data following the route of the ship. The closest point is obtained by finding the coordinates from the Arakawa-grid that have the smallest difference with respect to the compass position for each of the N couples of coordinates. The route does not appear like a smooth curve since the coordinates are not interpolated, therefore an interpolation between the points of the grid closest to the true position might be used to visually improve the results.

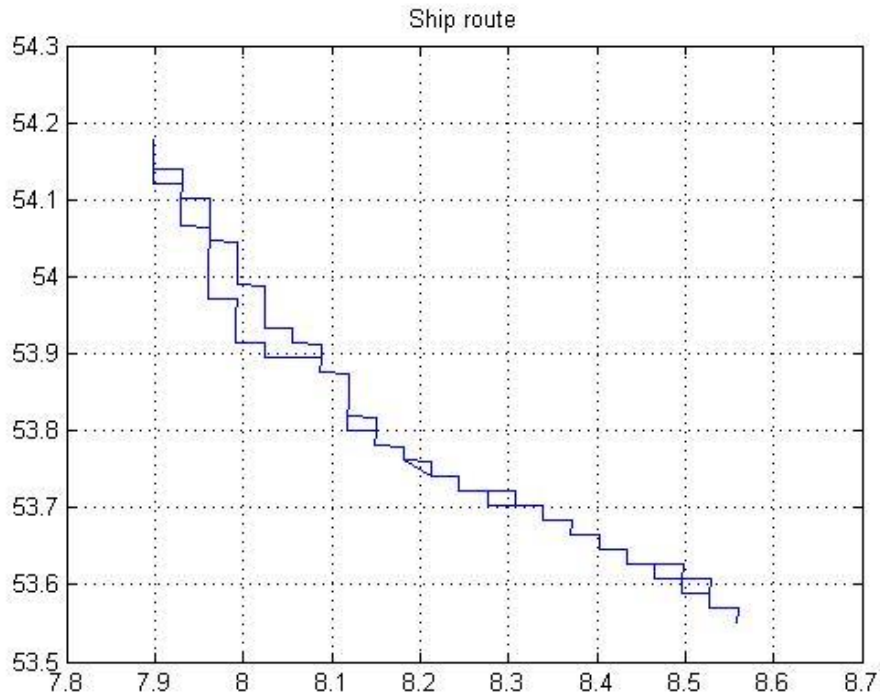


Figure 2.15: Route of the ship from Bremerhaven to Helgoland and way back on July 3 (non-interpolated samples).

In order to obtain a routine that compares the corrected lidar data and the simulation data, one needs to take into account both time- and space-related information.

The temporal information tell us that the WRF data provide a 30-min average wind speed while the lidar data give information each second. Therefore, these two sources need to be processed in order to be comparable. Since for every coordinate we get a wind speed value of the WRF data, the resulting N values need to be averaged in space. A simple average of the first 1800 values is done in order to obtain the 30-min wind speed value corresponding to the first 30 minutes where the ship was. In this way, the procedure provides a weighted average depending on where the ship mainly is.

This process has been implemented in the Matlab® code and works for the whole day. After it makes an average of the wind speed values considering the position of the ship in space as explained above, the routine skips every half an hour to the related WRF matrix that contains

the wind speed information corresponding to the next 30-min. The resulting WRF wind speed vector will have 48 values, each one related to a different time and position. Furthermore, the right cell in the vertical direction containing the measurement height needs to be found in order to determine the wind speed corresponding to the desired height, in this case 100 m. Because of the different pressure levels that change with time, the vertical index of the cell may vary on each time step [2]. So the cell needs to be detected every time step to find the closest values to the desired height. A further interpolation in height might be useful to improve the results.

Not only the WRF data must be processed, but also the lidar data. After the correction has been applied, the lidar data are processed with a 10-min moving average made every minute, as explained in chapter 2.2.2. The first point represents the average of the first ten minutes, the second one is shifted starting from the second minute and averaging the following ten minutes, and so on. In this way, starting from N points corresponding every second to a different position, the resulting data set gives 1440 points (one every minute per day) that contains the information of the 10-min average.

In order to make a temporal comparison, three of the 10-min values (starting from the first one every 10 values) corresponding to the 30-min time step of the WRF data need to be taken into account and therefore are averaged together. Thus, the resulting lidar wind speed vector contains 48 elements, each one corresponding to a 30-min average value. The results of this comparison are showed and further discussed in the next chapter.

3. CHAPTER III: RESULTS AND DISCUSSION

3.1. Results and assessment

This chapter is aimed at showing the results and findings of the work done and at discussing them in order to evaluate the scientific outcomes and the possible future research work. The main result obtained during this work is an approach for using the ship-lidar data within an offshore wind resource assessment. This approach, explained in the chapter related to the methodology, is the processing procedure that can be applied to the data recorded by a ship-based lidar system independently on the research campaign.

During this work, the Helgoland campaign and the FINO1 campaign have been the main means through which it has been possible to obtain a dataset to be used to evaluate the feasibility of this method. The question is therefore if it is possible to verify the approach and the answer can be obtained from the comparison with a reference, e.g. the met. mast FINO1. The following outcomes include the correlations values and the limits of the method with future possible improvements. A fundamental outcome of this research work is that the correction of the lidar data is mandatory for the ship-based lidar measurements.

The approach used for the processing of the lidar data can be used within offshore wind resource assessment and shows accurate results. For both campaigns, the correction procedure applied is the same but the comparison procedures change depending on the data sources. The data from the Helgoland campaign have been first processed and compared with the DWD dataset, which represents a rough comparison but shows a first good correlation, and afterward, another procedure and comparison have been carried out with the WRF dataset. The latter is a more elaborated procedure and gives results that are more detailed.

3.1.1. Post-processing procedure and example dataset from the Helgoland campaign

After the correction procedure has been implemented in Matlab, the whole dataset of the Helgoland campaign, i.e. from 2 June 2016 to 22 August 2016, has been processed. First, the motion correction and averaging process has been applied to single days and afterward to the whole dataset. Figures 3.1 and 3.2 show the uncorrected and corrected wind speed and direction for a sample day, the 22 August 2016. The red and blue curves represent the uncorrected and corrected data, respectively. It is possible to see a lower speed value during the stay of the ship in the port of Bremerhaven, oscillating between 5 m/s and 8 m/s. The corrected data show an increase in wind speed while the ship is offshore; the uncorrected data are clearly influenced by the rotation and velocity of the ship and the consequent change in wind direction.

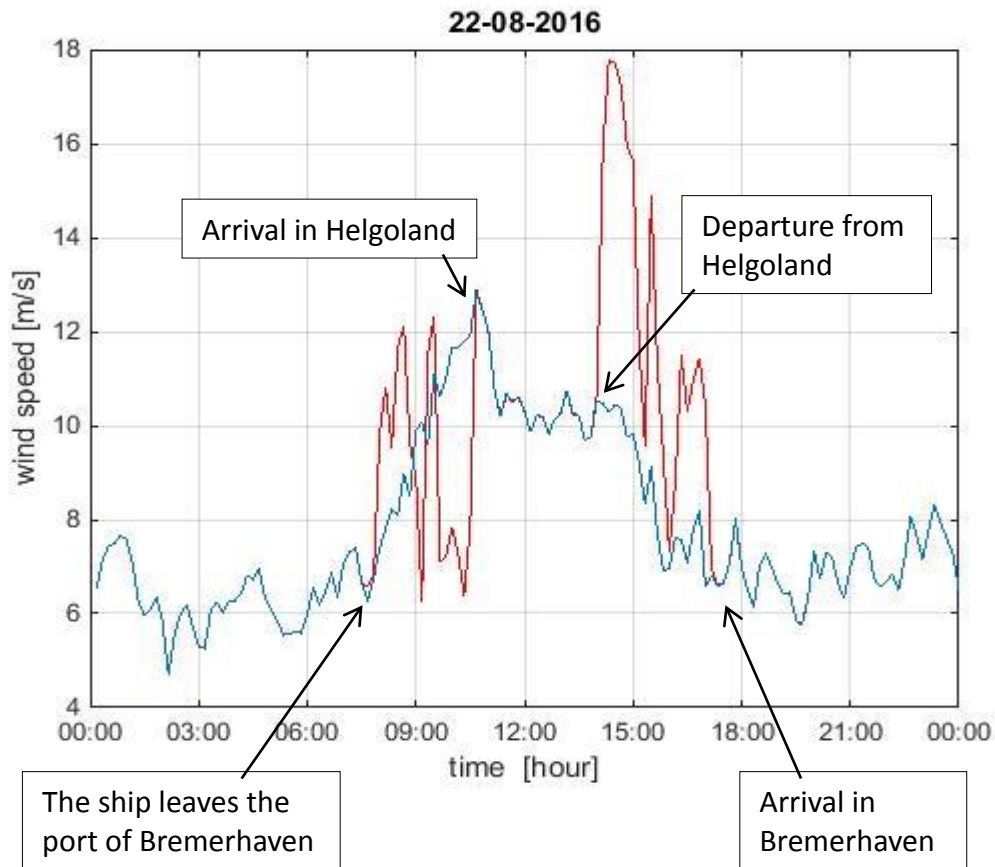


Figure 3.1: Comparison between corrected and uncorrected wind speed. The red curve represents the uncorrected data, which shows a clear influence of the ship movement; the blue curve corresponds to the corrected data, which show an increase of wind speed while the ship is offshore.

As well as for the wind speed plot, the direction trends show differences while the ship is moving (see Figure 3.2). In fact, during transit from Bremerhaven to Helgoland and vice versa, influences in the measured wind speed and direction dependent on ship and wind velocity can be identified. On the contrary, when the ship is moored, there are no variations between measured and corrected data, as expected. The only evidence is that there is still an offset between measured and corrected wind direction data when the ship is in the port, which can be known from the system configuration and setup but was not considered in this case.

Another consideration can be done in case the measured wind direction shows strong fluctuations. The reason for this is that the real wind velocity and ship velocity are quite similar. Since the measured wind velocity is a vector addition of both contributions, small variations in both terms results in high directional fluctuations of the resulting measured vector [10].

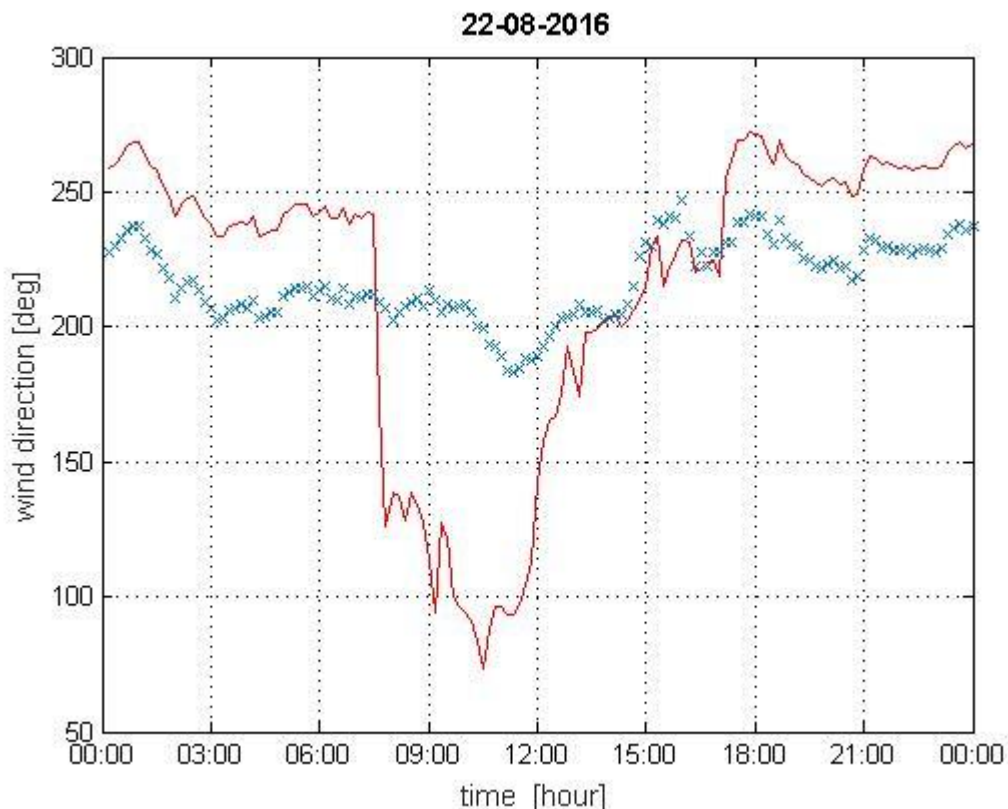


Figure 3.2: Comparison between corrected and uncorrected wind direction for the selected day. The red curve represents the uncorrected data, the blue one corresponds to the corrected data.

Thanks to the measurement principle of the Wind-Cube lidar, the measurements corresponds to the vertical wind profile in the height range from 40 to approximately 300 m simultaneously at several (of the order of 10) heights (see chapter 1.4). During this campaign, the wind data are measured from 42 m to 232 m every 10 m. Since the lidar is installed on the deck of the ship, the measurement heights are considered as 50 m height. Figure 3.3 shows the corrected lidar data for 03 August 2016 and three different heights: the blue one corresponds to 50 m, the green one to 100 m, and the red one to 150 m. As it is possible to see, the wind speed values increase with the height, according to the standard wind profile model.

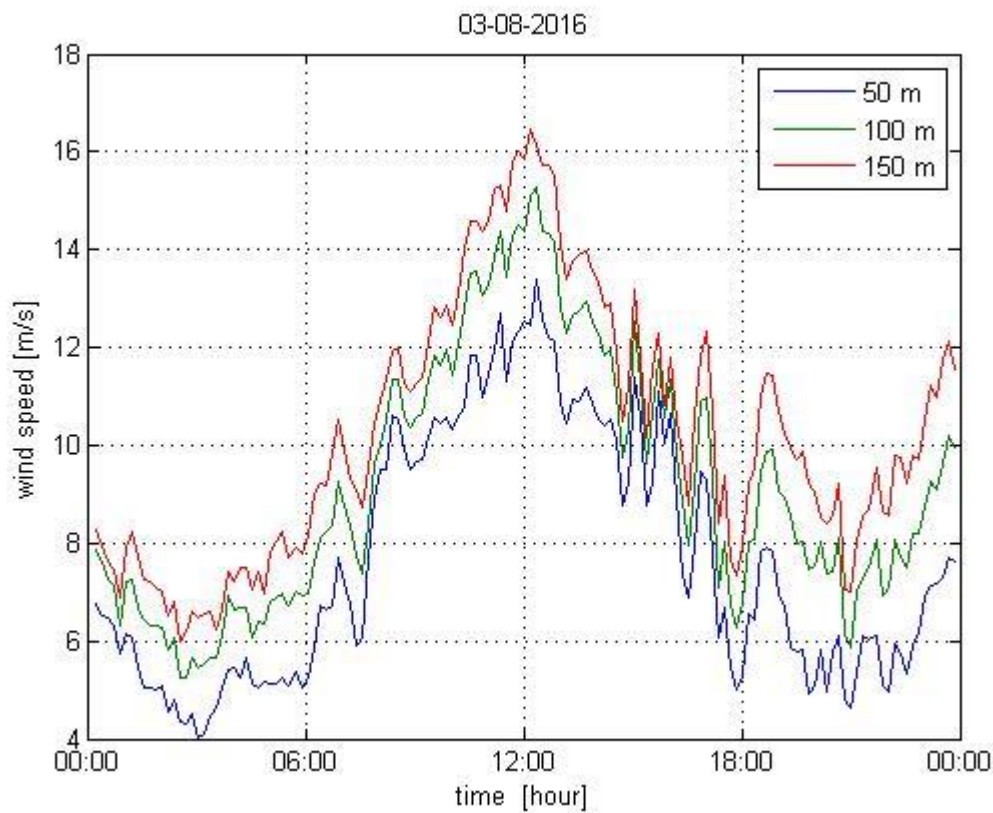


Figure 3.3: Corrected lidar data for 03 August 2016 and three different heights. The blue curve corresponds to 50 m, the green one to 100 m, and the red one to 150 m. The increase in height implies an increase in the wind speed as suggested from the wind profile.

Figure 3.14 shows the corrected dataset for the month of July. The value of the wind speed follows the same trend showed in the previous plots: it increases while the ship is offshore and stays in the port of Helgoland and decreases while the ship is moored in the port of Bremerhaven. The wind speed is included in the range between less than 1 m/s and reaches up to 18 m/s. The trends for the other available months can be found in Appendix A.

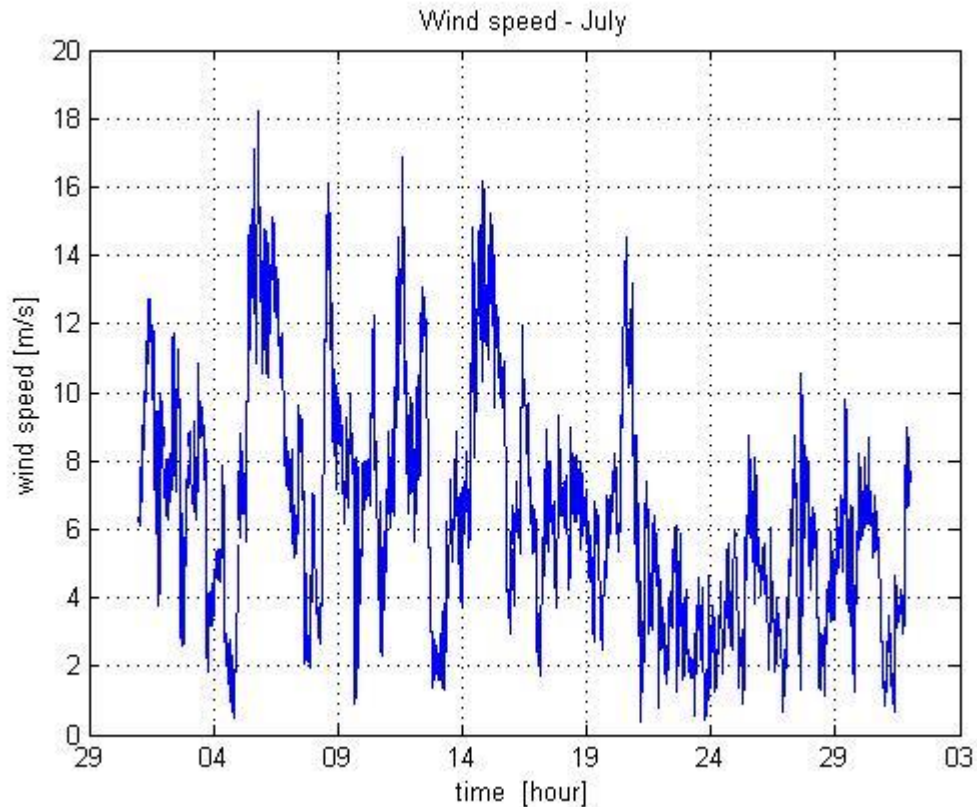


Figure 3.4: Wind speed trend for the whole month of July 2016 at 100 m height. The plot shows the corrected data. The value of the wind speed follows the same trend every day, increasing while the ship is offshore and decreasing while the ship is moored in the port of Bremerhaven.

3.1.2. Results and assessment of the Helgoland campaign

The preliminary comparison that has been carried out for the Helgoland campaign is with the data by German Weather Service (DWD). It is considered preliminary since the climatological time series available from the DWD database are hourly means of wind speed (in m/s) and direction (in degrees). Moreover the measurements are made at a lower height, and therefore the comparison is not fully consistent.

The procedure consists in representing the registered lidar data and the DWD data obtained from both the met. mast in Helgoland and Bremerhaven in the same plot. Figure 3.5 shows the comparison between the ship-lidar data and the DWD data for 22 August 2016. The figure shows the wind speed obtained from lidar measurements at a height of 50 m, while the met. masts in Bremerhaven and Helgoland have sensor heights above ground of 11.6 m and 10 m, respectively.

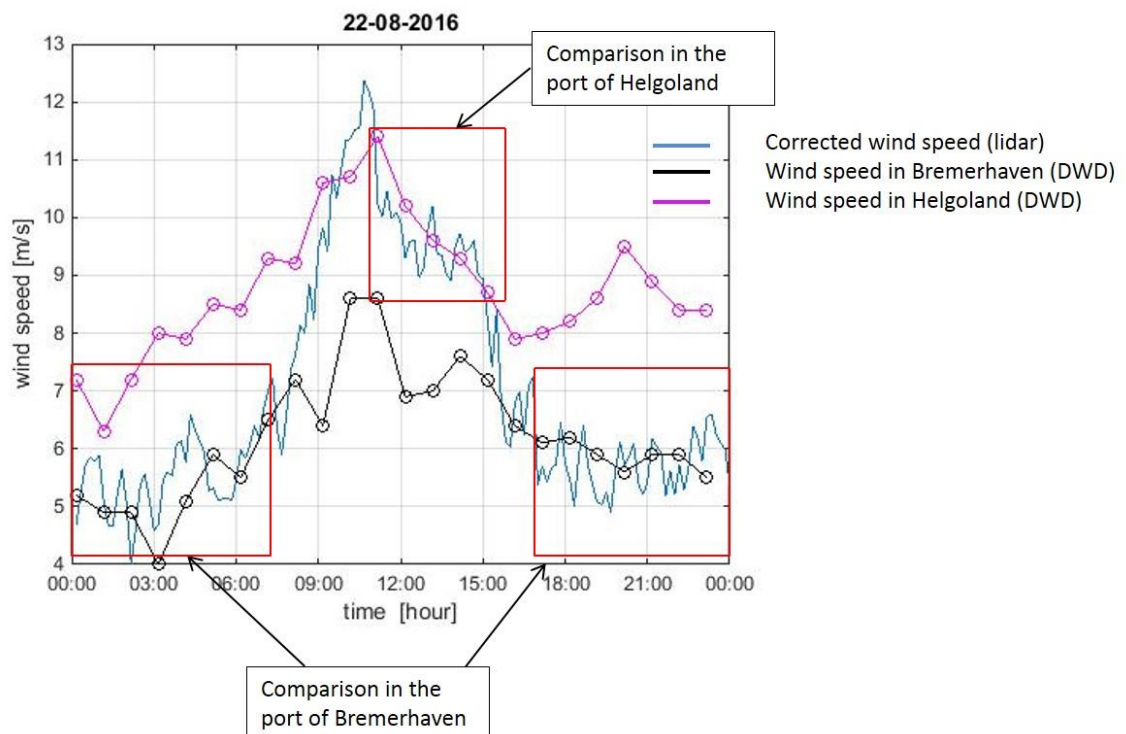


Figure 3.5: Comparison between the ship-lidar wind speed and the DWD wind speed time series. The figure shows the wind speed obtained from lidar measurements at a height of 50 m, while the met. masts in Bremerhaven and Helgoland have sensor heights above ground of 11.6 m and 10 m, respectively. The

climatological time series available from the DWD database are hourly means of wind speed (in m/s) and direction (in degrees); therefore, the comparison cannot be done more precisely.

The same comparison can be done for the wind direction. As well as the previous plot, figure 3.6 shows the trend of the wind direction for the wind lidar and both the met. masts in Bremerhaven and in Helgoland. A very similar trend can be seen in both ports. The blue line represents the corrected wind direction obtained from the lidar measurement, the black one is the registered wind direction in Bremerhaven and the pink one is the curve for wind direction registered in Helgoland.

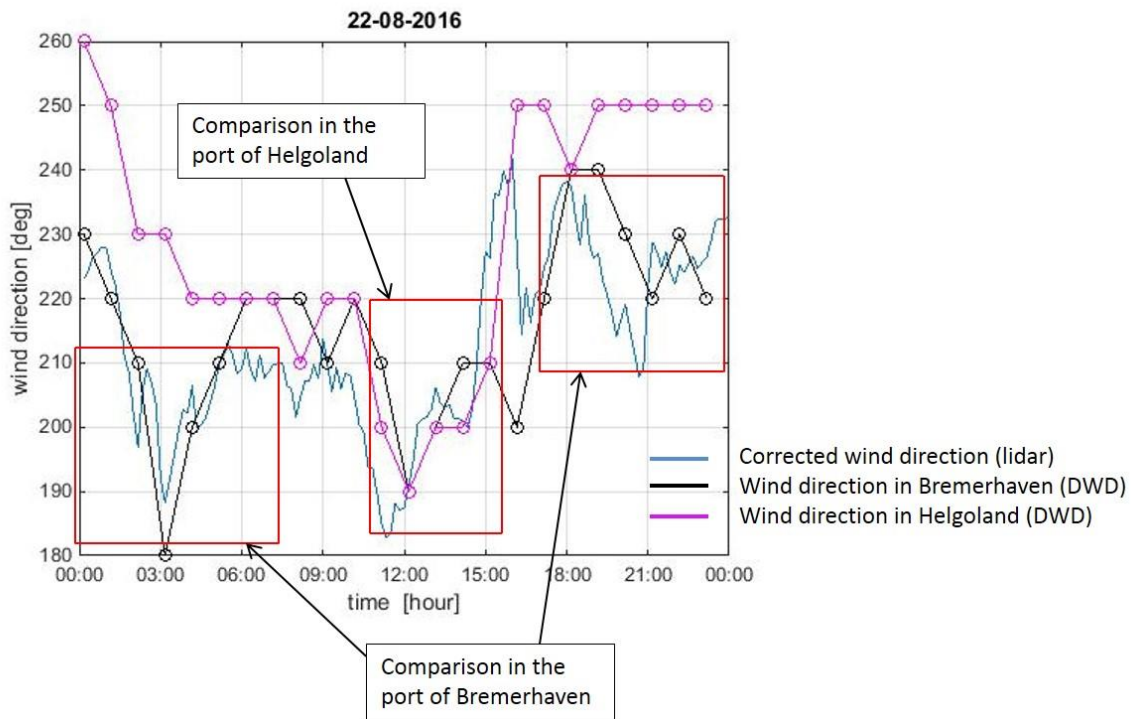


Figure 3.6: Comparison between the ship-lidar wind direction and the DWD wind direction values. The blue line represents the corrected wind direction obtained from the lidar measurement, the black one corresponds to the registered wind direction in Bremerhaven, and the pink one regards the same direction in Helgoland.

The following Figure 3.8 represents the comparison for 3 July 2016 for wind speed and direction, respectively. Here it is possible to see the high correlation between lidar and DWD data as well.

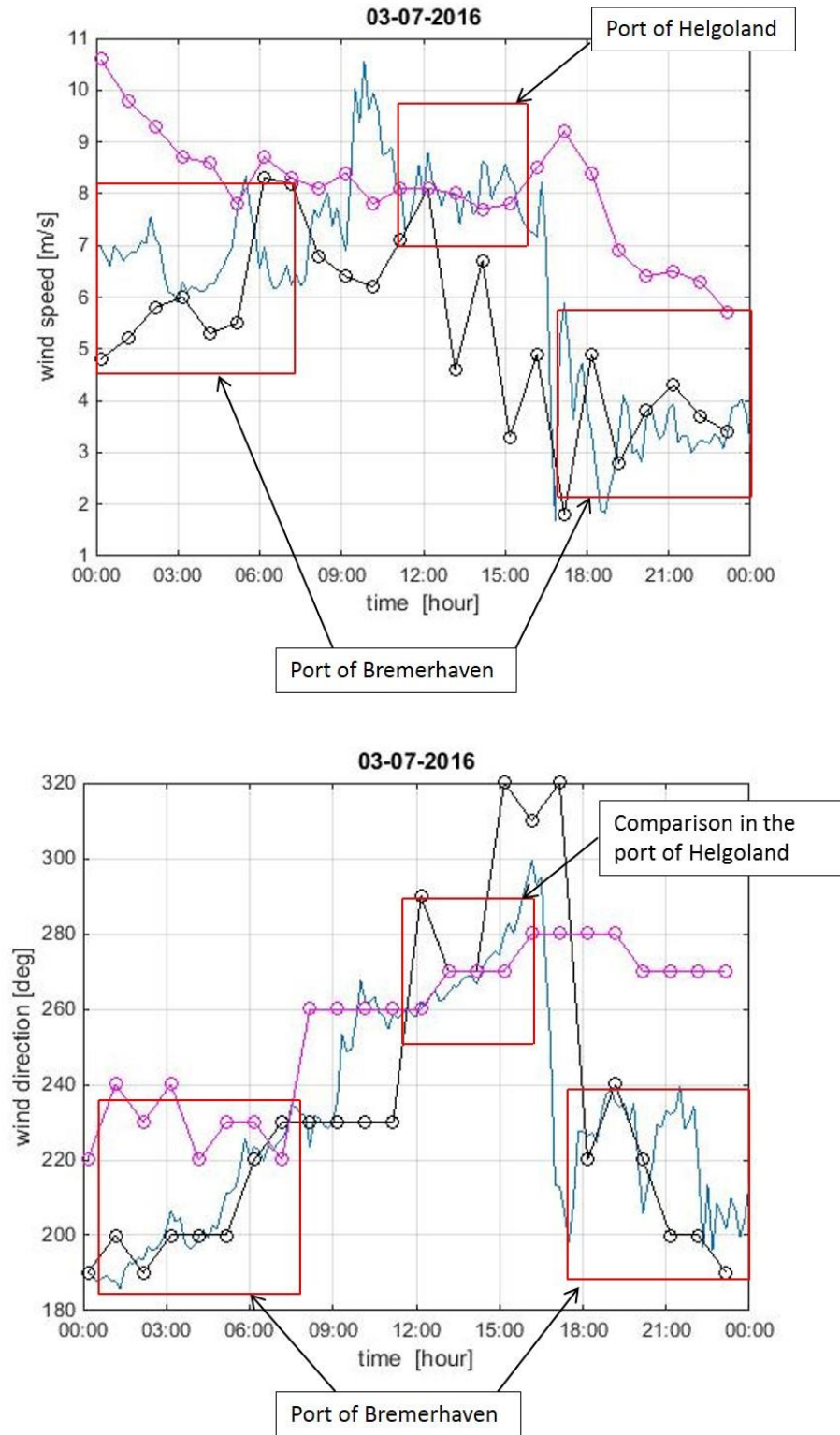


Figure 3.7: Comparison between the ship-lidar and the DWD wind speed and direction, respectively. The blue line represents the corrected values obtained from the lidar measurement, the black one corresponds to the registered wind direction in Bremerhaven, and the pink one regards the same direction in Helgoland.

The next step of the validation process has been between lidar data and WRF data. This procedure has been applied in a more detailed way compared to the comparison with DWD data. Here the results are presented and discussed, first for single days and afterward for the complete available dataset (complete details included in Appendix A).

The WRF data available for the comparison cover the whole month of July. A first step of the comparison is the evaluation of the relative deviation of the wind speed plotted over different hours of the day.

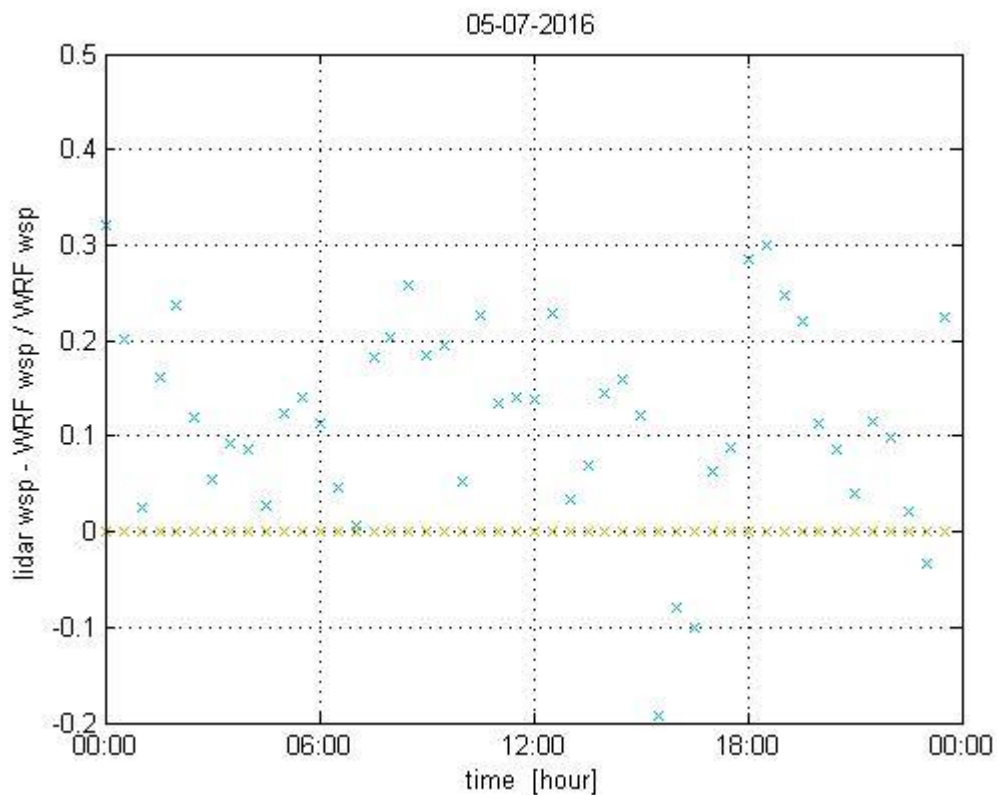


Figure 3.8: Difference between lidar wind speed and WRF wind speed. The plot shows a large deviation during the return trip from Helgoland to Bremerhaven between 3 pm and 6 pm.

Figure 3.8 shows the relative deviation between lidar and WRF data for 05 July. It is possible to notice that the deviation is included in a certain range but the largest effect is seen during the return trip of the ship (between 3 pm and 6 pm).

The lidar data have been processed following the simplified motion correction procedure and then prepared for the WRF comparison with the routine explained in Section 2.3.3. In Figure 3.9 it is possible visualize the track of the ship that has been obtained through this procedure by plotting a parameter representing the coordinate of the ship over time for 3 July 2016. This parameter is the value that corresponds to the position of the element in the indexing matrix. During nighttime, the ship is moored in Bremerhaven's port, then around 7 AM it goes to Helgoland, stays in the port, and comes back in the afternoon around 5 PM.

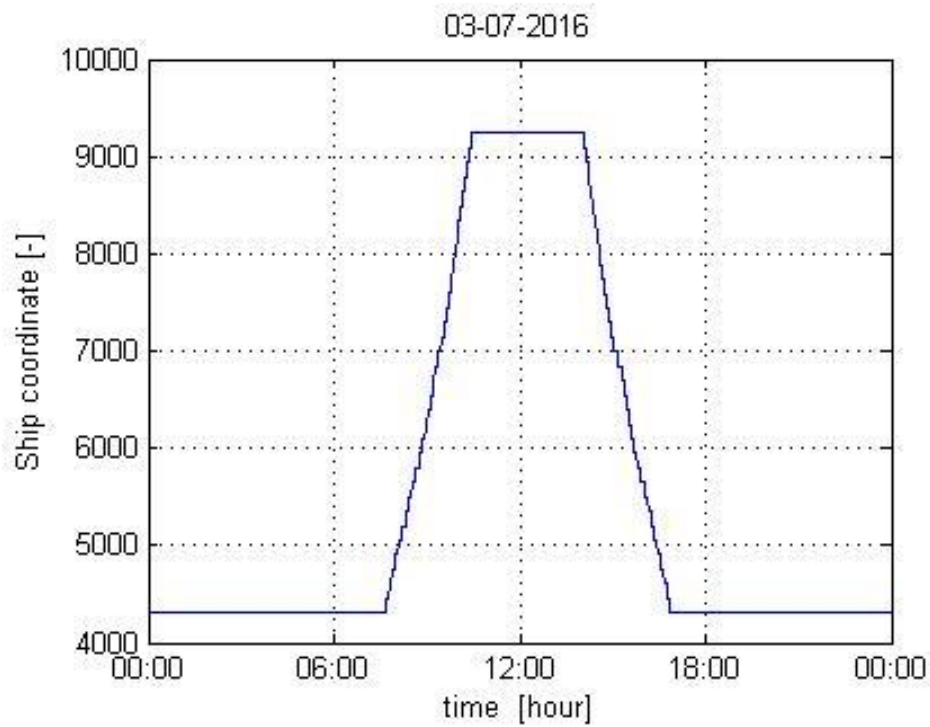


Figure 3.9: Coordinate of the ship plotted over time for the day 3 July 2016. It is possible to visualize that during nighttime the ship is moored in Bremerhaven's port, then around 7 AM it goes to Helgoland, stays in the port, and comes back in the afternoon.

Regarding the comparison between the WRF and lidar data, Figure 3.10 shows the wind speed trend for the sample day 3 July 2016. The red line represents the 30-min average value measured with the lidar; the blue one represents the WRF data (30-min value). It is possible to notice that the matching of the two estimates on the way to Helgoland looks accurate, while for the other times of the day the WRF data seem to overestimate the wind speed. This can be possible since the WRF data are the results of a simulation and not a measurement source. A smaller lidar wind speed for the time where the ship is in the harbor might be due to wake effects and the presence of building, which are not taken into account in simulations.

Furthermore, the two curves of Figure 3.10 needed to be shifted of half an hour in order to fit correctly. This is due to the fact that the lidar data have a timestamp at the start of the period (because of the averaging process), while the WRF data can be interpreted as if they correspond to the end of the interval. The comparison for two further sample days is presented in Figure 3.11.

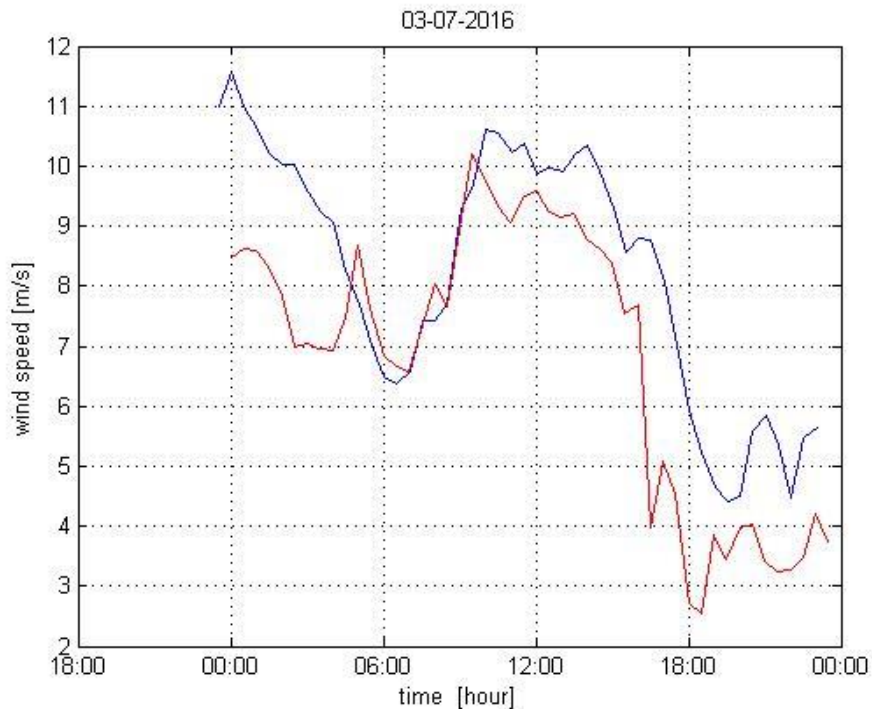


Figure 3.10: Wind speed over time for 3 July 2016. The red line represents the 10-min average value measured with the lidar; the blue one comes from the simulation data of the WRF model (30-min value). A high correlation on the way to Helgoland is showed and the whole trends look similar, despite the overestimation of wind speed by the WRF simulation.

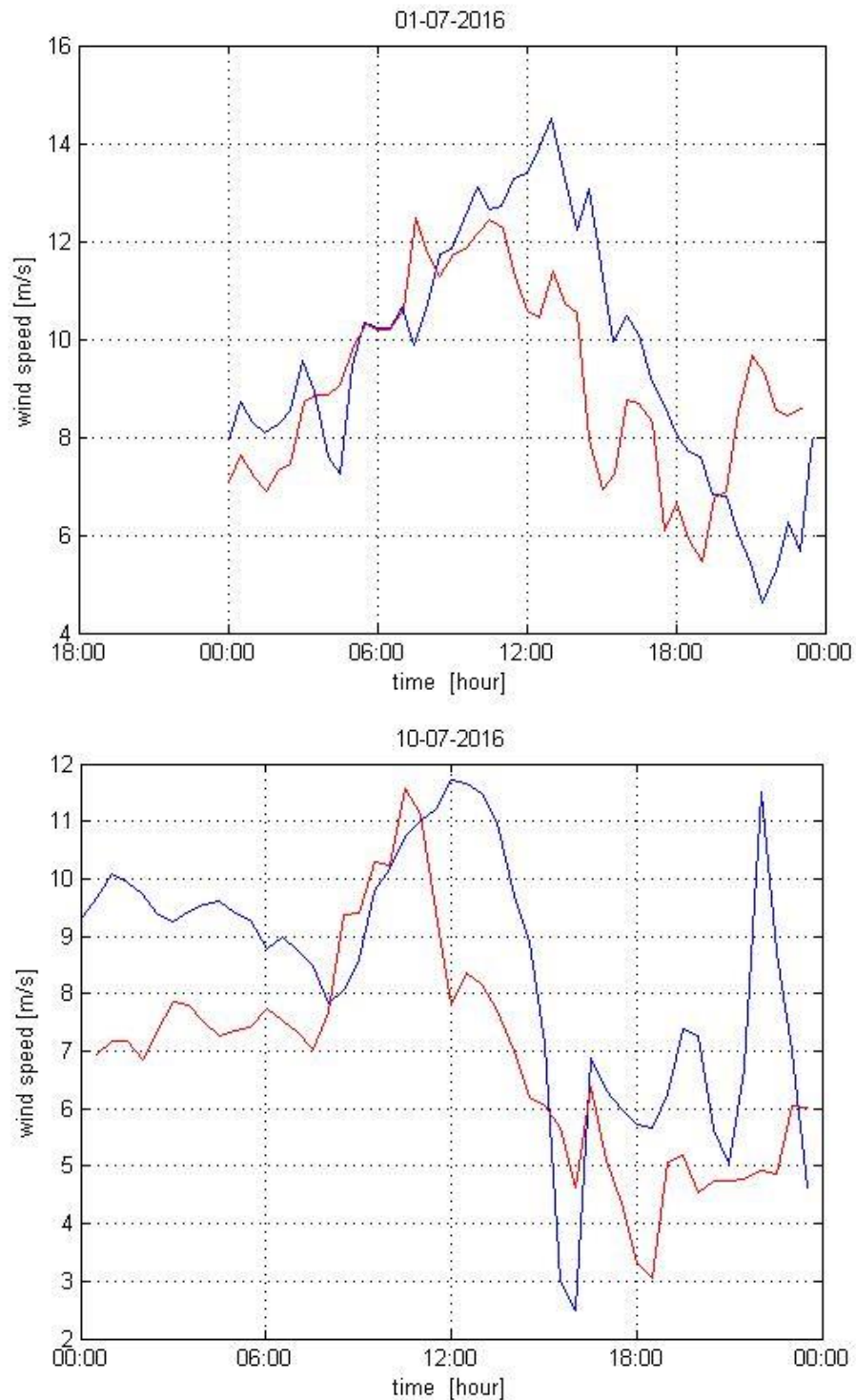


Figure 3.11: wind speed over time for 1 and 10 July 2016. The red line represents the 10-min average value measured with the lidar; the blue one comes from the simulation data of the WRF model (30-min value). A correlation on the way to Helgoland is showed and the whole trends look similar, despite the overestimation of wind speed by the WRF simulation. The second day looks shifted but it can be related to the uncertainty of the simulation data.

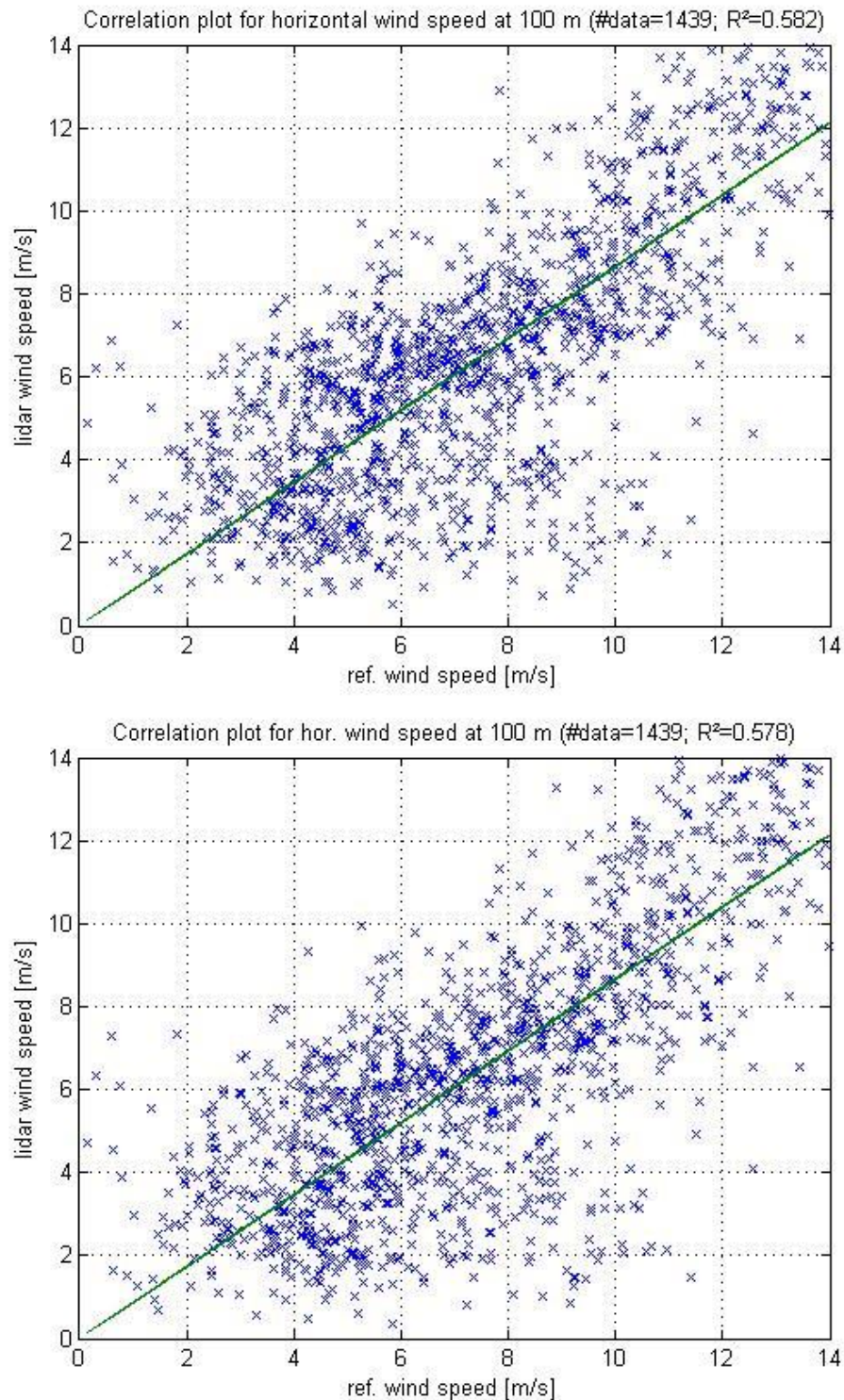


Figure 3.12: Correlation plots for wind speed values obtained by the lidar measurements and the WRF simulation. Top-figure: the lidar data have been processed with an average every 30 minutes. Correlation value $R^2 = 0.582$. Bottom-figure: only one value every 30 minutes of the lidar data has been taken into account. Considering the value centred at the end of the timestamp, $R^2 = 0.554$ while using the lidar value at the beginning and then shifting it of half hour gives $R^2 = 0.578$.

The two correlation plots for wind speed values between lidar and WRF data showed in Figure 3.12 are obtained as follows: in the first one, the lidar data have been processed with an average every 30 minutes, resulting in a correlation value $R^2 = 0.582$; in the second one only one value every 30 minutes of the lidar data has been taken into account. Considering the value centered at the end of the timestamp, $R^2 = 0.554$ while using the lidar value at the beginning and then shifting it of half hour gives $R^2 = 0.578$. The best fit is given by the 30-min average value and therefore is the one considered for the next evaluations.

Since for some days the wind speed trend looks similar during the trip to Helgoland, it has been chosen to evaluate the correlation value only for specific times. In Figure 3.13 the correlation plot between the 30-min average wind speed from lidar measurements and the WRF simulation from 7:00 to 11:00 am is shown, by restricting to the times when the ship is moving from the port of Bremerhaven to Helgoland. The resulting correlation value is $R^2 = 0.678$.

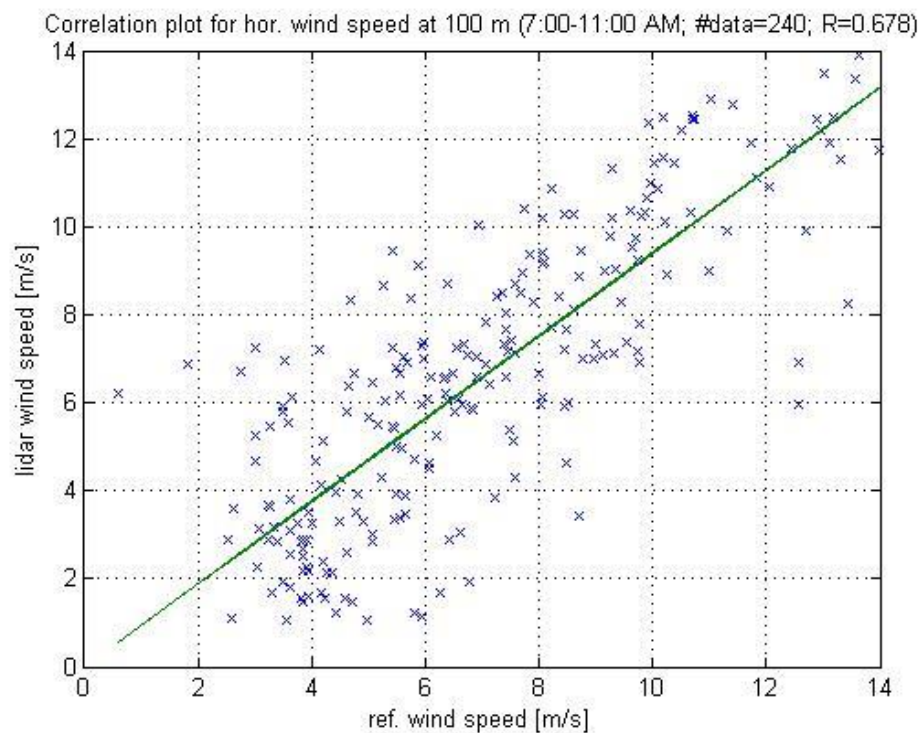


Figure 3.13: Correlation plot between 30-min average wind speed from lidar measurements and the WRF simulation. The hours taken into account are from 7:00 to 11:00 am only when the ship is moving from the port of Bremerhaven to Helgoland. Correlation value $R^2 = 0.678$.

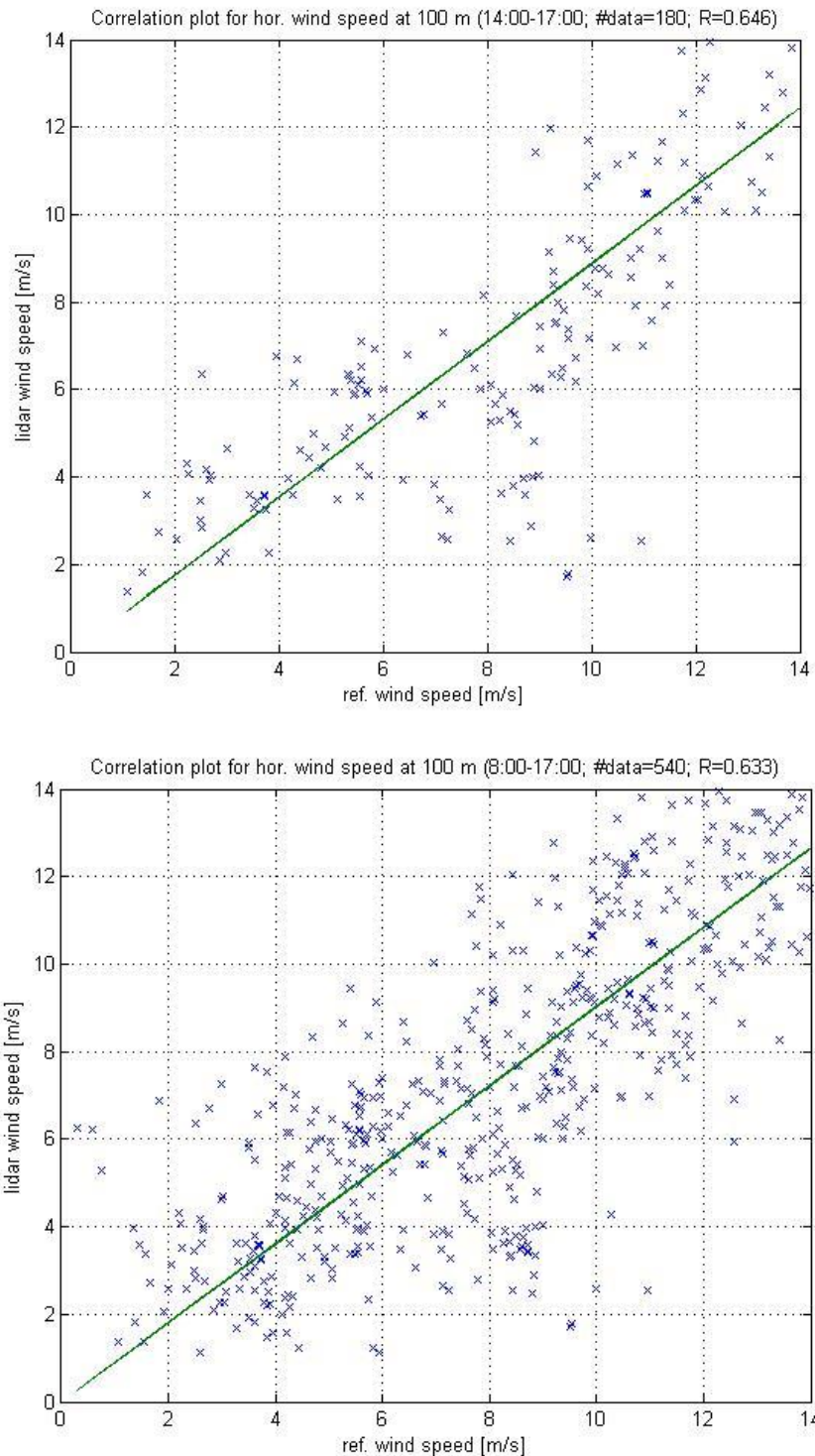


Figure 3.14: correlation between 30-min average wind speed from lidar measurements and the WRF reference. Top-figure: the hours taken into account are from 2:00 to 5:00 PM, only when the ship is moving from the port of Helgoland to Bremerhaven; correlation value $R^2 = 0.646$. Bottom-figure: the hours taken into account are from 8:00 AM to 5:00 PM, only when the ship is moving from the port of Helgoland to Bremerhaven. Correlation value $R^2 = 0.633$.

It can be seen that the measured and the simulated values deviate from each other. Despite the similar trend that is showed in Figures 3.10 and 3.11, the WRF model tends to overestimate wind speed, which affects the fit between the two results, as suggested by the correlation values.

These results are summarized in Tables 3.1 and 3.2. Table 3.1 shows the influence of the time step chosen for the lidar mean on the resulting coefficient of determination. It is possible to see that, the time of the day and the number of data being equal, the 30-min mean gives higher correlation with the WRF simulation; therefore, this choice has been used for the other correlations. Table 3.2 contains only 30-min mean values and shows the selected time of the day, the number of data, and the correlation coefficient.

<i>Lidar data mean</i>	<i>Time of the day</i>	<i>#data</i>	<i>R²</i>
10-min	Whole day	1439	0.578
30-min	Whole day	1439	0.582

Table 3.1: influence of the time step chosen for the lidar mean on the resulting coefficient of determination.

<i>Time of the day</i>	<i>#data</i>	<i>R²</i>
<i>Whole day</i>	1439	0.582
<i>7 AM – 11 AM</i>	240	0.678
<i>2 PM – 5 PM</i>	180	0.646
<i>8 AM – 5 PM</i>	540	0.633

Table 3.2: results from lidar-WRF comparison for 30-min mean lidar values. The first column shows the time of the day taken into account for the comparison; the second shows the number of data selected and the third one the corresponding coefficient of determination.

3.1.3. Results, assessment and sensitivity for the FINO1 campaign

After the outcomes of the Helgoland campaign have been discussed, the results of the FINO1 campaign are presented as well, in order to show the applicability of the procedure in different campaigns. Figures 3.15 and 3.16 show wind speed and wind direction trends for the sample day 11 June 2014, respectively. The red line represents the wind speed value measured with the lidar before the correction has been applied; the blue one represents the corrected lidar data (10-min average); the black line corresponds to the FINO1 wind speed; and the pink one represents the corrected lidar data only when the ship is close to the met. mast (distance $d < 2$ km). The plots show a very good matching between the two data sources.

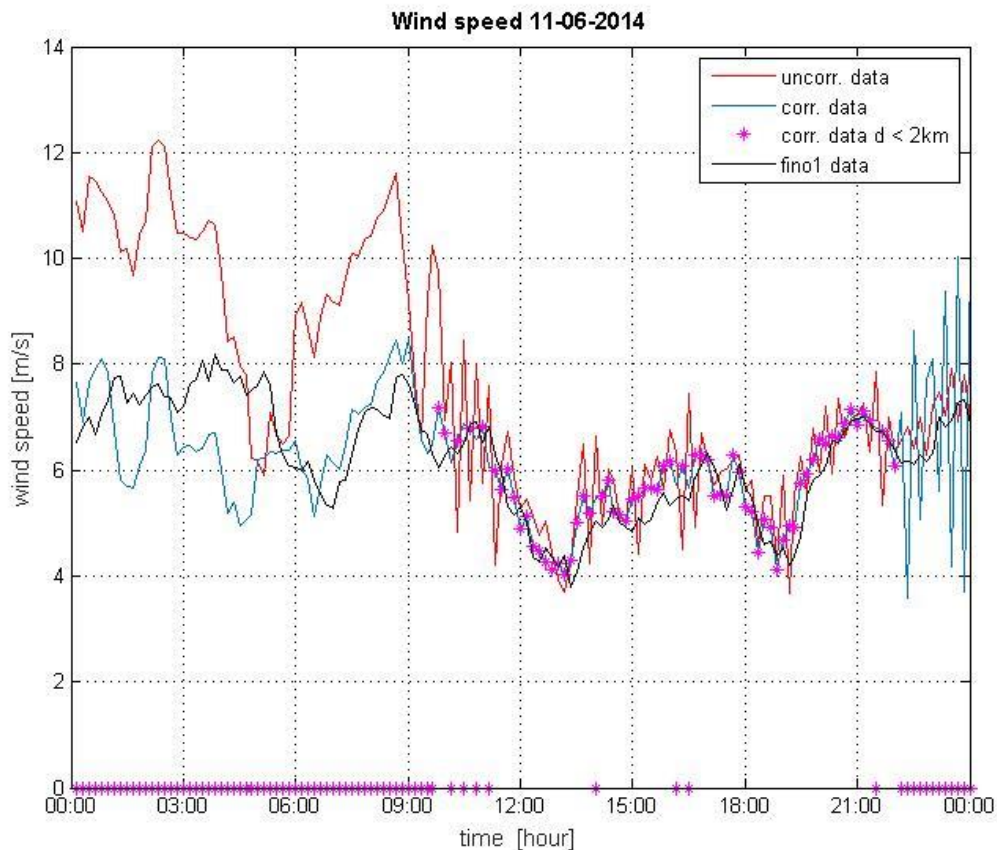


Figure 3.15: Wind speed for the sample day 11 June 2014. The red line represents the wind speed value measured with the lidar before the correction has been applied; the blue one represents the corrected lidar data (10-min average); the black line corresponds to the FINO1 wind speed; and the pink one represents the corrected lidar data only when the ship is close to the met. mast (distance $d < 2$ km; when the distance is larger than 2 km, a dummy zero value is shown).

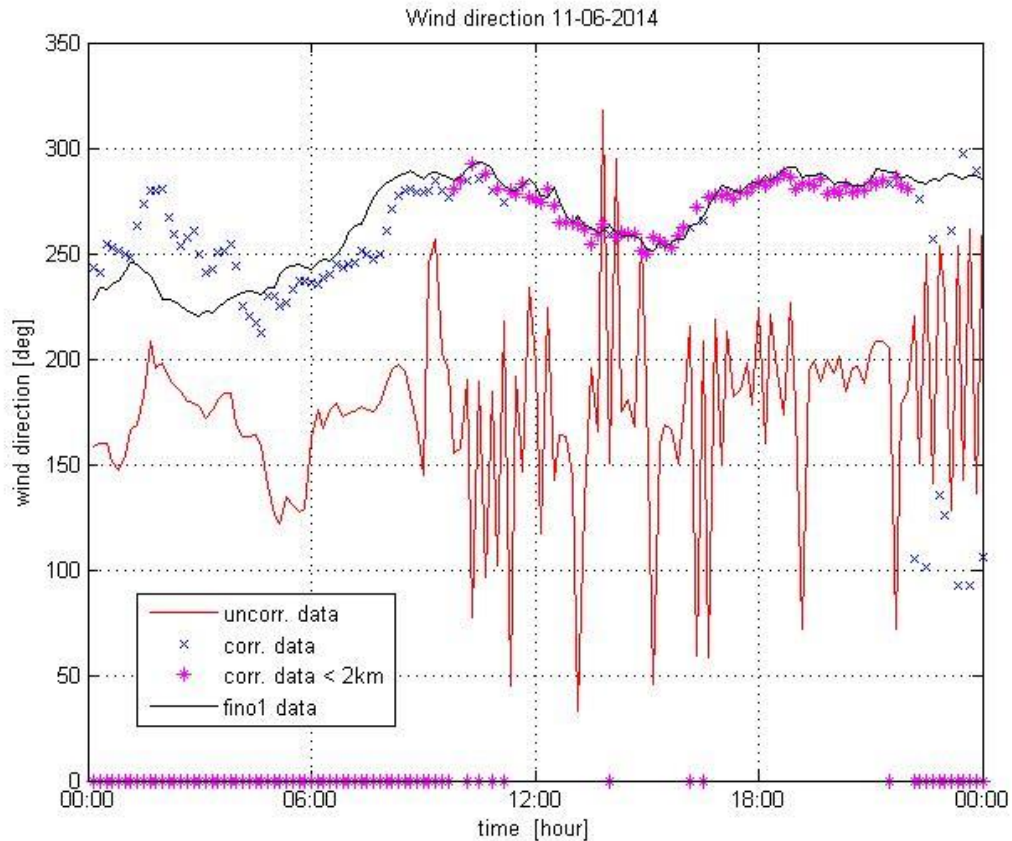


Figure 3.16: Wind direction for the sample day 11 June 2014. The red line represents the wind speed value measured with the lidar before the correction has been applied; the blue one represents the corrected lidar data (10-min average); the black line corresponds to the FINO1 wind speed and the pink one represents the corrected lidar data only when the ship is close to the met. mast (distance $d < 2$ km; when the distance is bigger than 2 km, a dummy zero value is shown).

The accuracy of the measurements of horizontal wind speed by the floating lidar system (FLS) is assessed by performing a linear-regression analysis on the FLS and reference data.

The following Figures 3.17 and 3.18 show the results for the two measurement heights of 100 m and 60 m, respectively. The blue crosses correspond to 10-min-mean values; the red line represents the linear fit as result of one-parameter linear-regression analysis, the yellow line regards the linear fit with the intercept. The resulting coefficients of determination show a very high correlation between the two data sources at both heights.

The derived parameters for the linear fit – slope and coefficient of determination, together with the number of evaluated data points – are summarized in Table 3.2.

<i>Height [m]</i>	<i>#data</i>	<i>slope</i>	<i>R²</i>
100	248	1.0098	0.984
60	151	0.9958	0.983

Table 3.3: results from data assessment for lidar measurements of wind speed in the FINO1 campaign.

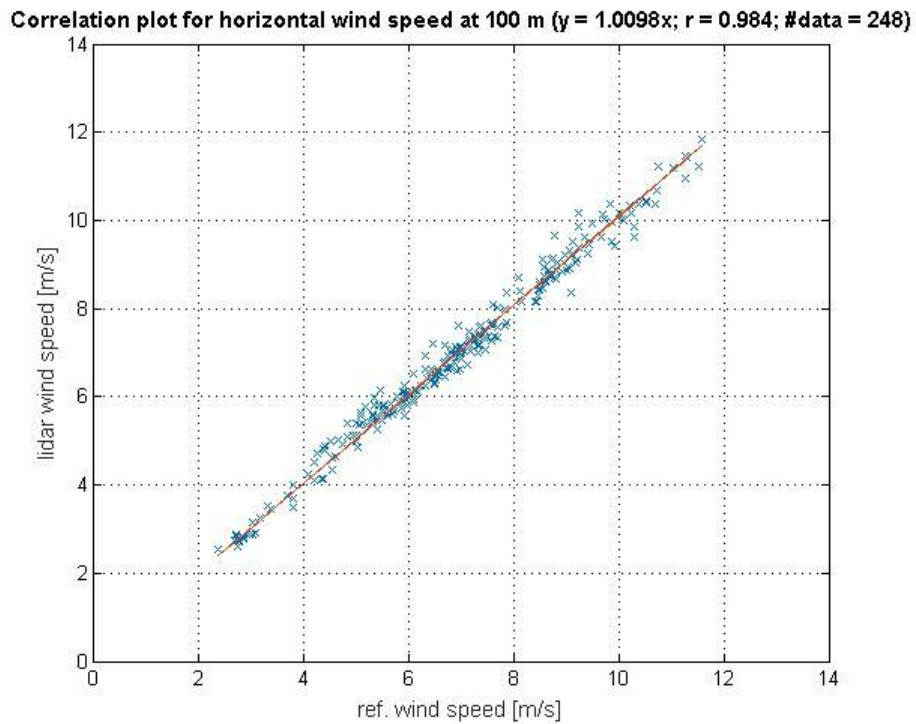


Figure 3.17: Correlation plot for measurements of horizontal wind speed at 100 m. The blue crosses correspond to 10-min-mean values; the red line represents the linear fit as a result of one-parameter linear-regression analysis.

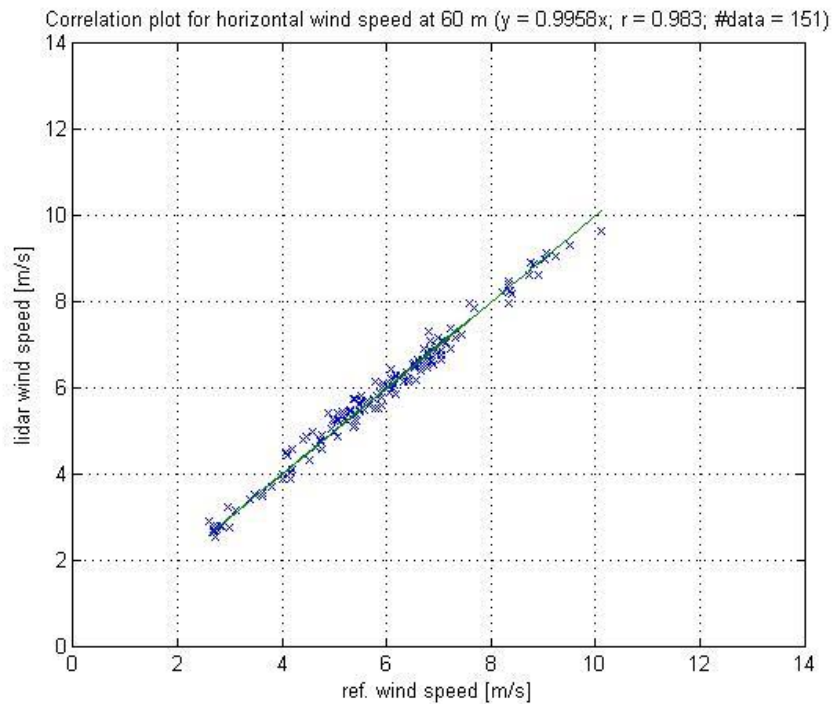


Figure 3.18: Correlation plot for measurements of horizontal wind speed at 60 m. The blue crosses correspond to 10-min-mean values.

This first sensitivity study takes into account the deviations in measured wind speed at 100 m height in relation to the simultaneously recorded ship velocity and distance between the ship and the reference. As it is shown in Figures 3.19 and 3.20, no significant sensitivity is seen.

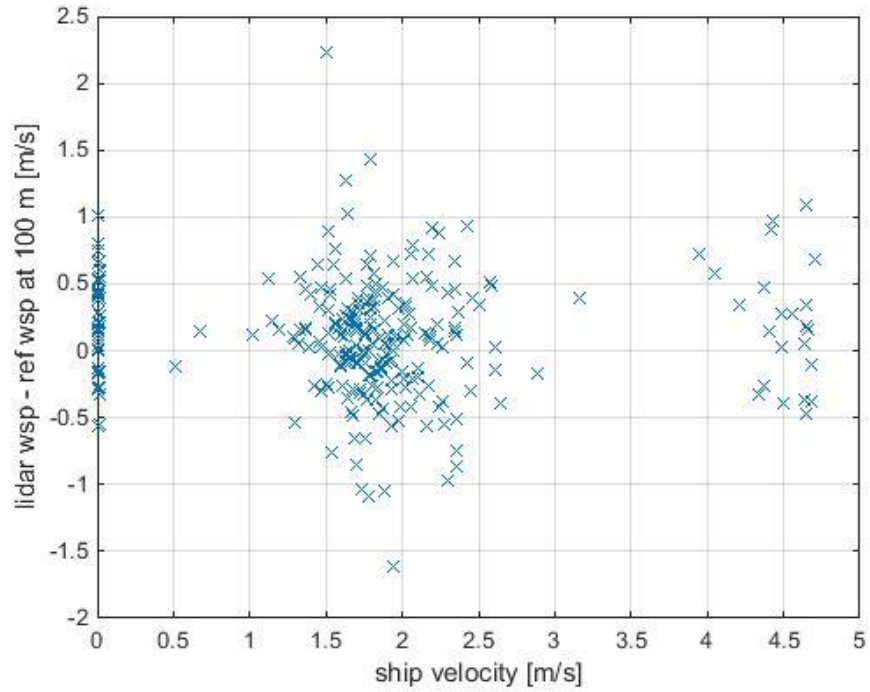


Figure 3.19: Sensitivity study: difference between the wind speed measured by lidar and the reference speed measured by the sensor at 100 m versus the ship speed.

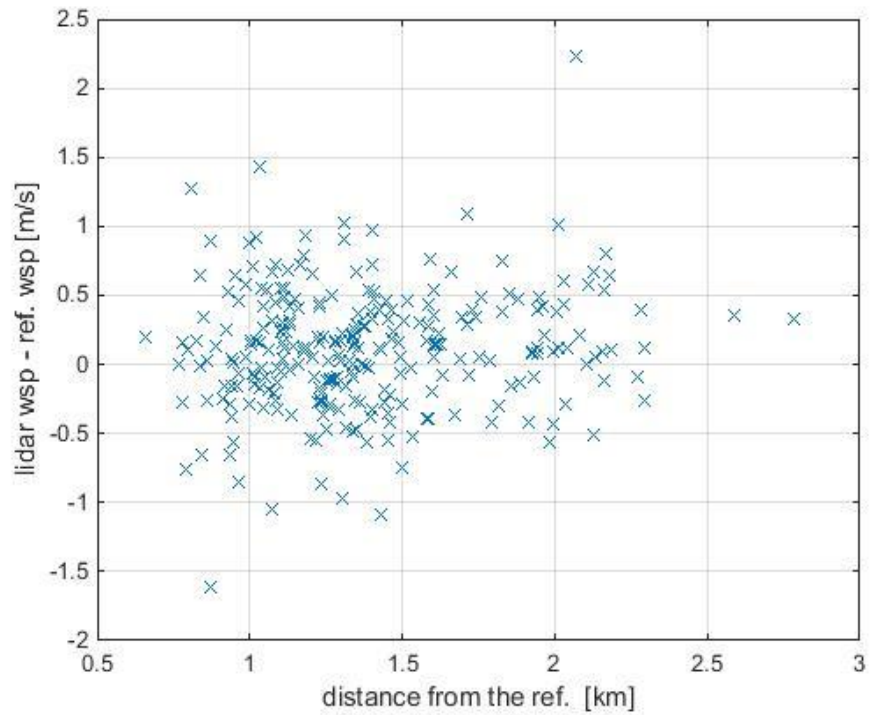


Figure 3.20: Sensitivity study: difference between the wind speed measured by lidar and the reference speed measured by the sensor at 100 m versus distance from FINO1.

3.1.4. Discussion on usability and feasibility of the final approach

The final approach obtained as an outcome of this thesis is related to the processing procedure that can be applied to ship-based lidar data in order to make them an accessible and usable source of information for the wind energy market. The experimental validation described in the previous sections demonstrates that it is possible to use a lidar system not only on fixed positions or buoys, but also on moving platforms such as ships and ferries.

On one hand, the essential element of this process is the correction of the registered data, since it is necessary to consider the translatory motion of the ship. On the other hand, the results of this work also suggests that, in this first approach, the rotation of the ship can be neglected. In order to obtain these results and verify the feasibility of the proposed approach, the Helgoland campaign and the FINO1 campaign have been used as main data sources and the relative met. masts have been used as the reference source. In both cases, the correction procedure used is the same, and therefore the results suggest that the proposed approach may be usable for different kinds of applications.

Regarding the FINO1 campaign, the comparison between corrected lidar data and the reference data have showed a very good result, with a coefficient of determination $R^2 = 0.984$. During the Helgoland campaign, the lidar data have been compared with are the DWD dataset, which represents only a preliminary, rather rough, comparison but shows a rather high correlation nonetheless, and the WRF dataset, which implies a more elaborated procedure and gives more detailed results .

Through the final formulation of the proposed approach, it has been possible to obtain these results independently on the lidar campaign. The only process that changes depending on the campaign is the comparison procedure, which of course is related to the nature of the data source that were available in each case for the comparison. Therefore, the aforementioned results suggest that the approach can be used for the processing of the lidar data within offshore wind resource assessment during the next campaigns.

3.2. Outlook and future research work

The results described in the previous sections show that the methodology applied to the ship-based lidar data has a high usability potential but still need some improvements, not only in terms of processing of the data but also for future applications.

From this perspective, the first step that could be addressed following this thesis is the improvement of the routine that allows the comparison between lidar and WRF data. Two kinds of interpolation of the WRF simulation results can be applied: the first one is relative to the horizontal grid of the WRF data and would permit to obtain a smooth curve for the track of the ship through the cells of the grid (see Figure 2.14); the second one is related to the height of the cell. By interpolating in height and obtaining the wind speed value at the effective desired height, the results would likely further improve because of the considerable influence of the wind profile.

Considering the routine used for the lidar – WRF comparison, it is possible to exploit a similar code to compare the lidar data with a satellite source. The process would be implemented in a similar way but it would not consider the change in time, since the satellites provide image time series of the interested area with a much sparser time sampling (of the order of days or weeks depending on mission and spatial resolution) than the other sources considered here. Nevertheless, a comparison can be done with, for example, the data coming from the TerraSAR-X mission, which has a high spatial resolution of 200 m. Therefore, this kind of comparison could provide further information on the relative accuracy of the lidar and satellite radar estimates of wind speed. A fundamental step of this process would be to develop the wind speed profile in order to extract the desired one, since the satellite data usually only provide the values at 10 m height.

A future research step, which is actually already underway, is another measurement campaign carried out on a ferry in the Baltic Sea with the same ship-based lidar system. This will allow of course more progresses in this research field by providing new datasets for the interested area and further research material.

CONCLUSIONS

The technology of ship-based lidar systems allows collecting precise wind speed measurements offshore and is a flexible alternative for a number of application areas, especially now that the number of planned wind farm projects is constantly growing. Compared to conventional methods such as fixed met masts or lidar devices on buoy or fixed platforms, a lidar system installed on a ship makes for easier maintenance and installation and lower costs. Another clear advantage of this new technology is the possibility to install the system on an already existent route that covers the location of interest. Nevertheless, the ship velocity and rotational movements influence the recorded data and therefore need to be considered and corrected.

During the work of this thesis, an approach for using the ship-lidar data within an offshore wind resource assessment has been developed and experimentally evaluated. This proposed approach includes both the aforementioned crucial step of motion correction and a moving averaging process aimed at making lidar data smoother, less noisy, and more accurate. The proposed approach has been experimentally validated with the data from two campaigns, FINO1 and Helgoland. For both campaigns, the correction procedure applied was the same but the procedures for the comparison between lidar-based wind speed measurements and other wind speed data sources vary depending on the individual sources that were available within each campaign.

The outcomes of the comparison for the FINO1 campaign have showed a very high coefficient of determination $R^2 = 0.984$ for a 100 m height and $R^2 = 0.983$ for a 60 m height, between lidar-based and met. mast measurements of wind speed, when selecting the lidar data for a distance smaller than 2 km between the ship and the met. mast. This result confirms the expected high accuracy of the lidar instrument in the measurement of wind speed and is consistent with earlier results obtained in previous analysis [16]. Furthermore, a first sensitivity analysis showed that no significant sensitivity is remarked with respect to the recorded ship velocity and distance between the ship and the reference. This further suggests the reliability of the proposed approach.

Regarding the Helgoland campaign, the correction has been applied for both wind speed and direction and a preliminary comparison with weather datasets shows agreement between the two data sources. Moreover, a specific routine for the comparison of lidar data with data from the WRF weather simulation model has also been developed for the Helgoland campaign. This routine represents a further outcome of this work in itself and allows remarking a good correspondence between the trends of the two different data sources, although the coefficients of determination is lower than for the FINO1 campaign. This is due to an overestimation of the wind speed by the WRF model. Indeed, it is worth recalling that, for the Helgoland campaign, the two benchmark data sources used for comparison were not direct measurements of wind speed (like in the previous case of the FINO1 campaigns) but were wind speed estimates in themselves. Therefore, disagreements with respect to the results of the proposed lidar-based approach are also affected by the intrinsic inaccuracies of these benchmark estimators.

With respect to the applicability of the considered new measurement system, on one hand, a ship-based solution results to be a good choice especially when a measurement is needed for a short period only and if a vessel in proximity to the location of interest is available; in this way, it can be used as a direct tool for offshore wind assessment. On the other hand, another possibility would be to exploit the ship-lidar system as a validation of a model to be used for wind resource assessment. This system represents an innovative solution compared to conventional measurements since it provides time series of data in both time and space and, thanks to the motion correction, can be reliable and easier to access.

The validation of the method have showed accurate results especially as compared with true *in-situ* measurements; these results suggest to proceed with future works and improvements along this research line; however, the developed procedure can be already used on an already existent route that corresponds to the location of interest and provide useful and accurate datasets.

REFERENCES

1. Wolken-Möhlmann, Gerrit e Gottschall, Julia. Ship Lidar System for Offshore Wind Measurements. *Fraunhofer IWES*. [Online] [Cited: 04 03 2017.] http://www.windenergie.iwes.fraunhofer.de/content/dam/windenergie/en/documents/Factsheets_english/Datenblatt%20Schiffs-Lidar-System_Engl_web.pdf.
2. Martens, Christine. *Filling of Gaps in LiDAR Buoy Measurements by Mesoscale Simulations (Master's thesis)*. Oldenburg: s.n., 2016.
3. *Guidelines for wind resource assessment: best practices for countries initiating wind development*. Bank, Asian Development. s.l.: ADB, 2014. 978-92-9254-563-5.
4. New European Wind Atlas . *NEWA*. [Online] [Cited: 20 02 2017.] <http://www.neweuropeanwindatlas.eu/>.
5. Troen, Ib and Lundtang Petersen, Erik. European Wind Atlas. *DTU Orbit - The research information system*. [Online] 1989. [Cited: 21 02 2017.] <http://www.orbit.dtu.dk>.
6. American Wind Energy Association . *AWEA*. [Online] [Cited: 23 02 2017.] <http://www.awea.org/>.
7. Goyer, G. G. e Watson, R. The Laser and its Application to Meteorology. *Bulletin of the American Meteorological Society*. 1963.
8. Pena Diaz, Alfredo, et al. *Remote Sensing for Wind Energy*. s.l.: DTU Wind Energy , 2015. 0084(EN).
9. Engelbrecht, Bilke. *Impact of data gaps on wind data statistics, with a special focus on offshore measurement data from a floating LIDAR system (Master report)*. s.l.: DTU Wind Energy, 2016. M-0114.
10. Gerrit Wolken-Möhlmann, Julia Gottschall, Hristo Lilov, Bernd Schillo, Thomas Viergutz, Bernhard Lange. *SHIP BASED LIDAR MEASUREMENTS*. Fraunhofer IWES, Bremerhaven, Germany: s.n.

11. *Ship-based lidar measurements in the wake of an offshore wind farm*. Wolken-Möhlmann, Gerrit and Gottschall, Julia. D5.5, DTU Wind Energy, Risø Campus, Denmark : s.n., 2014.
12. Hasager, Charlotte Bay. Offshore winds mapped from satellite remote sensing. *WIREs Energy and Environment*. 2014, Vol. 3, 3:594–603.
13. The weather research and forecasting model. *WRF Model*. [Online] [Cited: 03 03 2017.] <http://www.wrf-model.org/index.php>.
14. G. Wolken-Moehlmann, J. Gottschall, B. Lange. First verification test and wake measurement results using a ship-LIDAR system. *ScienceDirect*. [Online] 2014. [Cited: 02 02 2017.] <http://www.sciencedirect.com>.
15. Forschungsplattformen in Nord- und Ostsee Nr.1. *FINO1*. [Online] [Cited: 03 03 2017.] <http://www.fino1.de/en>.
16. G. Wolken-Möhlmann, J. Gottschall, B. Lange. A detailed analysis of ship-lidar measurements with comparison to FINO1. *EERA-DTOC*. [Online] 2015. [Cited: 04 03 2017.] http://www.eera-dtoc.eu/wp-content/uploads/files/DEWEK_Wolken-Moehlmann_poster_ADDED.pdf.
17. Moving Average. *Wikipedia*. [Online] [Cited: 05 03 2017.] https://en.wikipedia.org/wiki/Moving_average.
18. Trianel Windpark Borkum. *Wikipedia*. [Online] [Cited: 05 03 2017.] https://en.wikipedia.org/wiki/Trianel_Windpark_Borkum.
19. Deutscher Wetterdienst. *DWD*. [Online] [Cited: 19 10 2016.] https://werdis.dwd.de/werdis/start_js_JSP.do.
20. How to interpret WRF variables. *Open WFM*. [Online] [Cited: 06 03 2017.] http://www.openwfm.org/wiki/How_to_interpret_WRF_variables.
21. *Floating Lidar Systems: Current Technology Status and Requirements for Improved Maturity*. Gottschall, Julia. Hamburg: s.n., 2016.

22. A. SATHE, J. MANN, J. GOTTSCHALL, M. S. COURTNEY. Can Wind Lidars Measure Turbulence? *JOURNAL OF ATMOSPHERIC AND OCEANIC TECHNOLOGY*. 2011, Vol. 28.

Appendix A – Results of the Helgoland campaign

In this section the corrected dataset for the months of June and August of the Helgoland campaign can be found in order to show the complete dataset that was already discussed in Section 3.1.

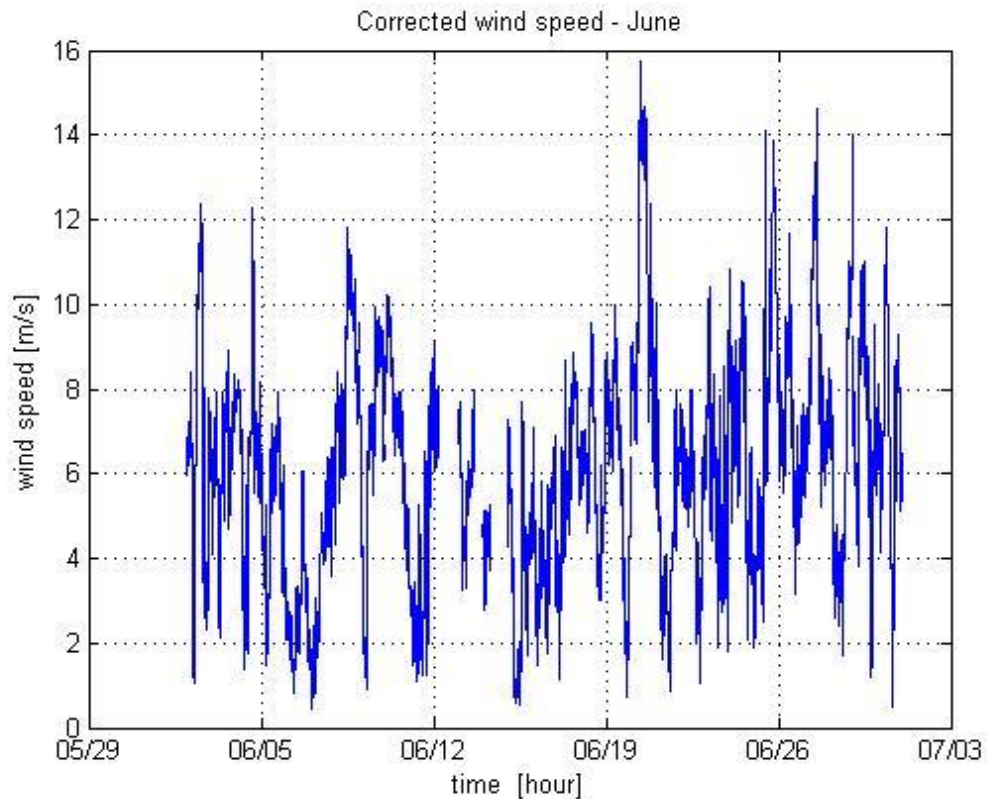


Figure A.1: Wind speed trend for the whole month of June 2016 at 100 m height. The plot shows the corrected data.

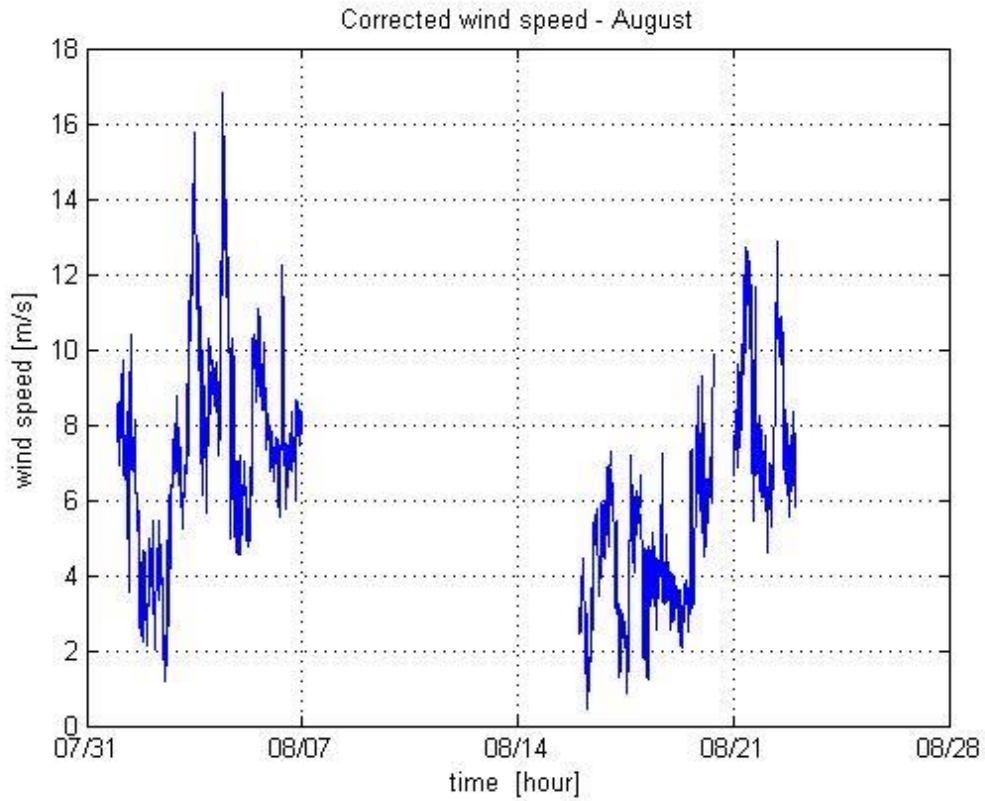


Figure A.2: Wind speed trend for the whole month of August 2016 at 100 m height. The plot shows the corrected data only for the available days.

Furthermore, every single day from the lidar-WRF comparison are presented.

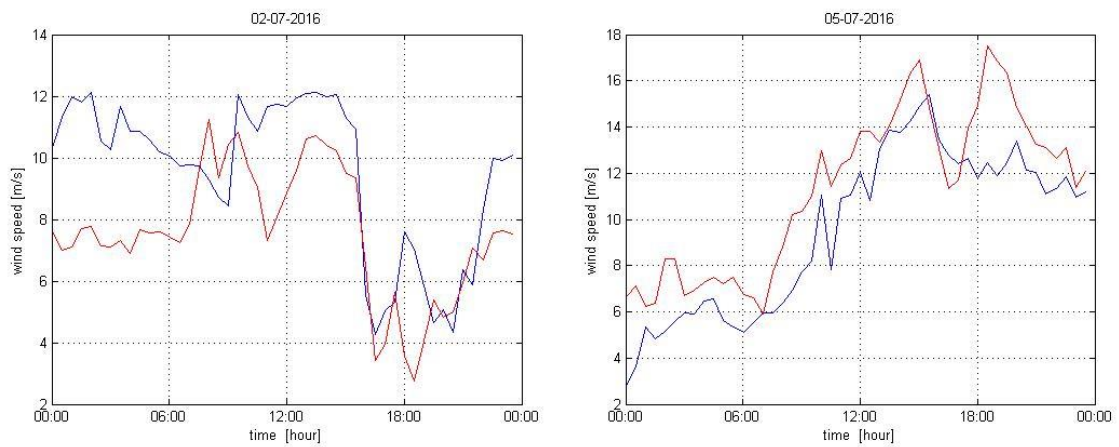


Figure A.3: Wind speed over time for the days 2 and 5 July 2016. The red line represents the 10-min average value measured with the lidar; the blue one comes from the simulation data (30-min value).

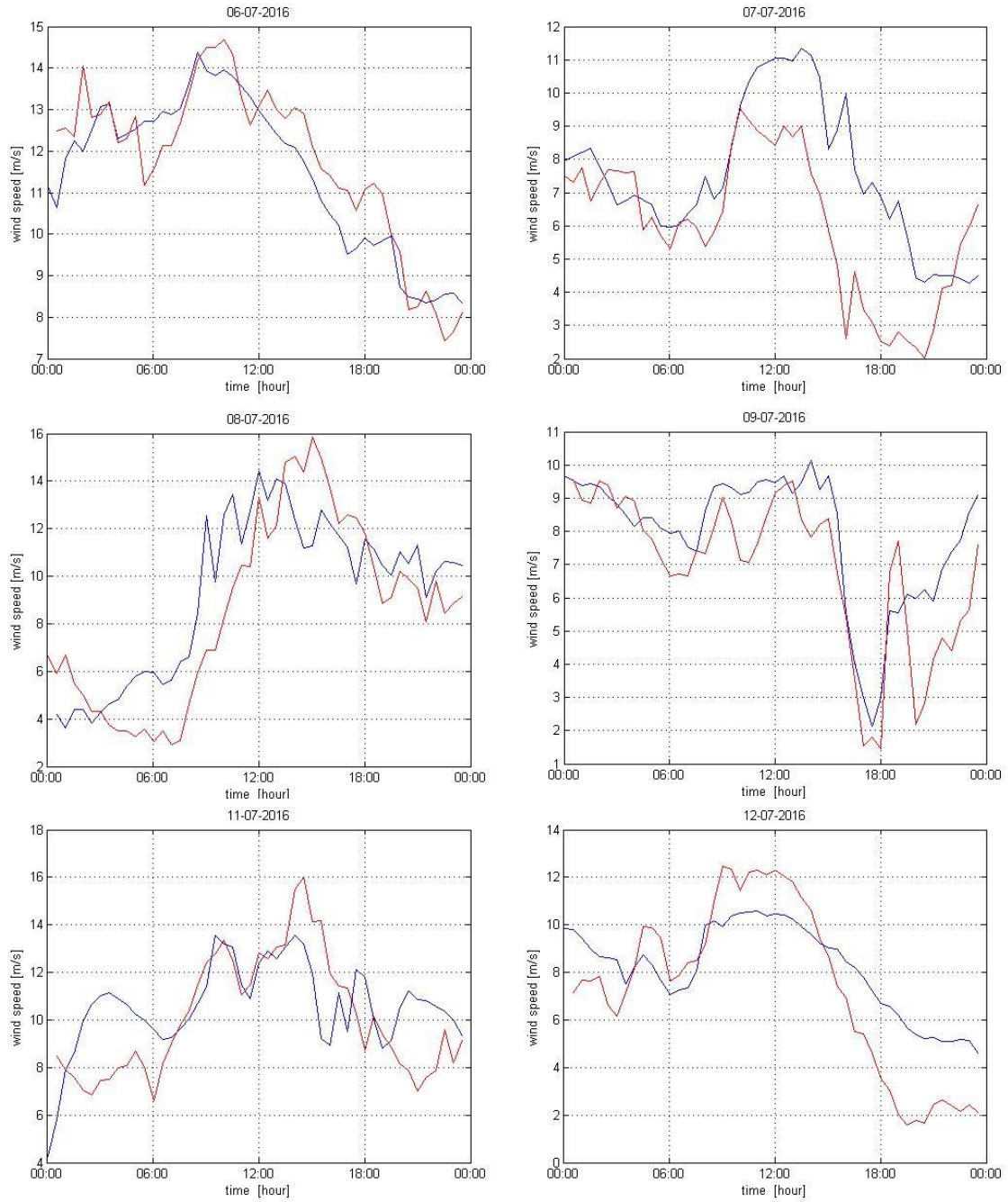


Figure A.4: Wind speed over time for the days 6 – 7 – 8 – 9 – 11 – 12 July 2016. The red line represents the 10-min average value measured with the lidar; the blue one corresponds to the simulation data (30-min value).

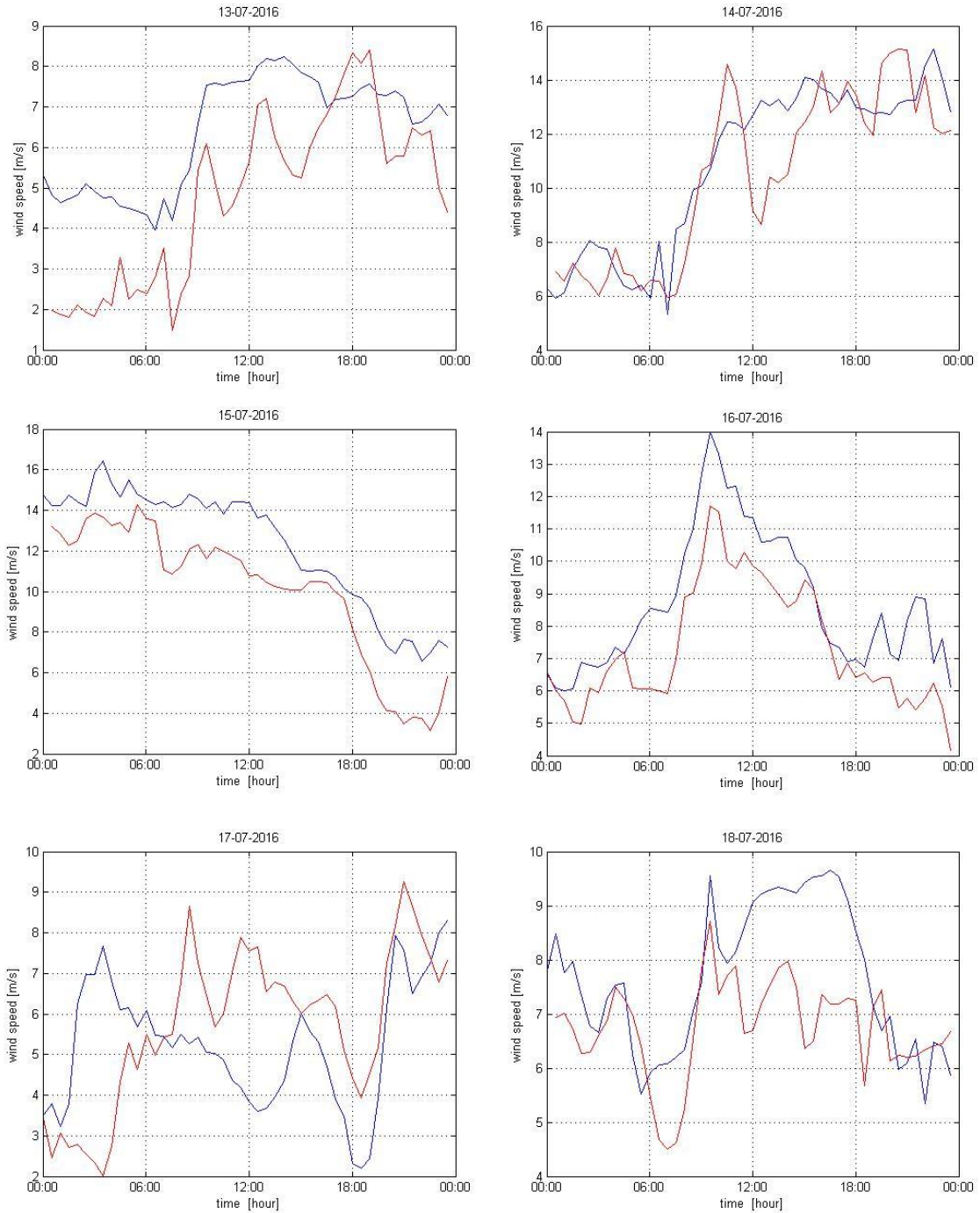


Figure A.5: Wind speed over time for the days 13 – 14 – 15 – 16 – 17 - 18 July 2016. The red line represents the 10-min average value measured with the lidar; the blue one corresponds the simulation data (30-min value).

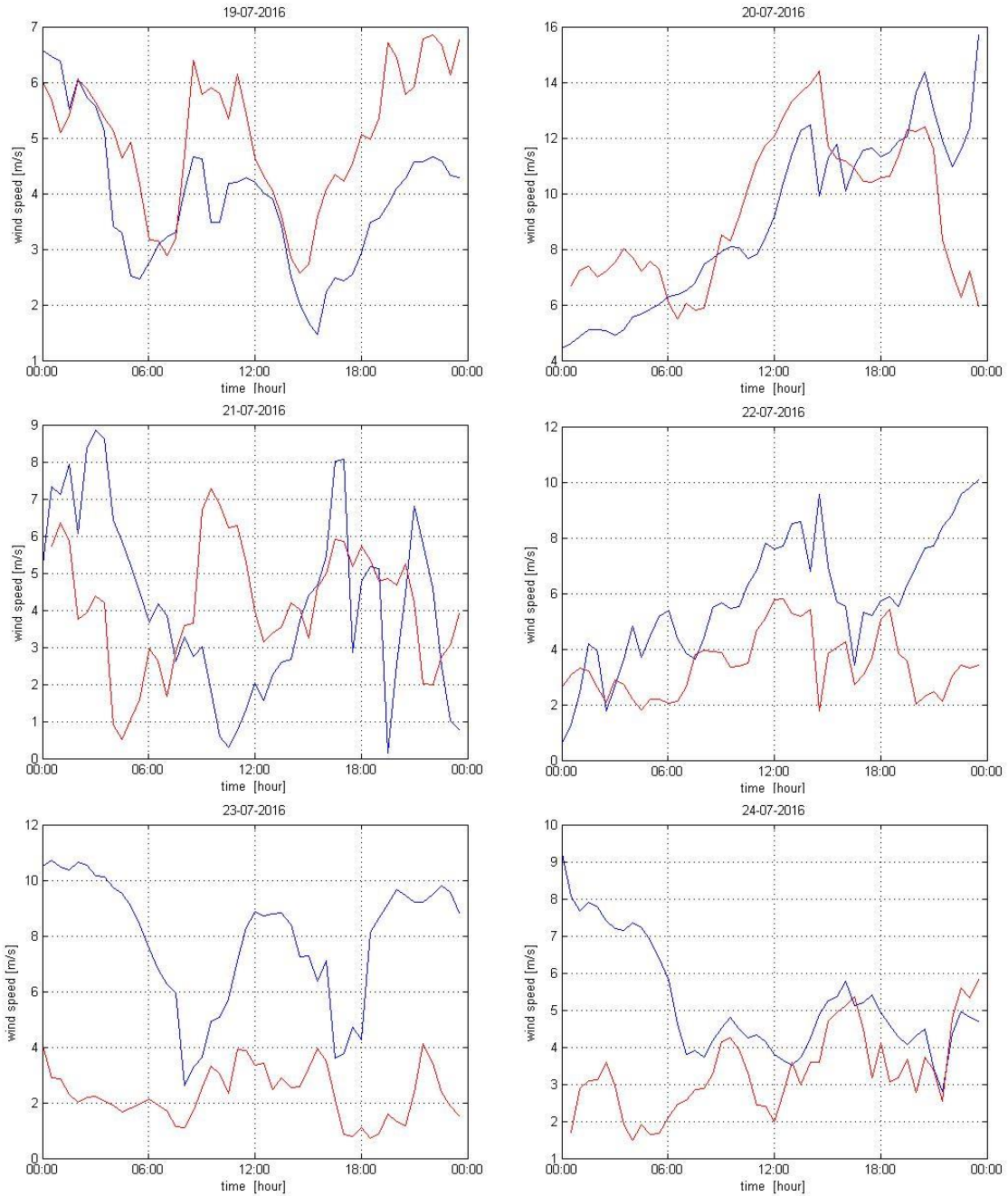


Figure A.6: Wind speed over time for the days 19 – 20 – 21 – 22 – 23 – 24 July 2016. The red line represents the 10-min average value measured with the lidar; the blue one corresponds to the simulation data (30-min value).

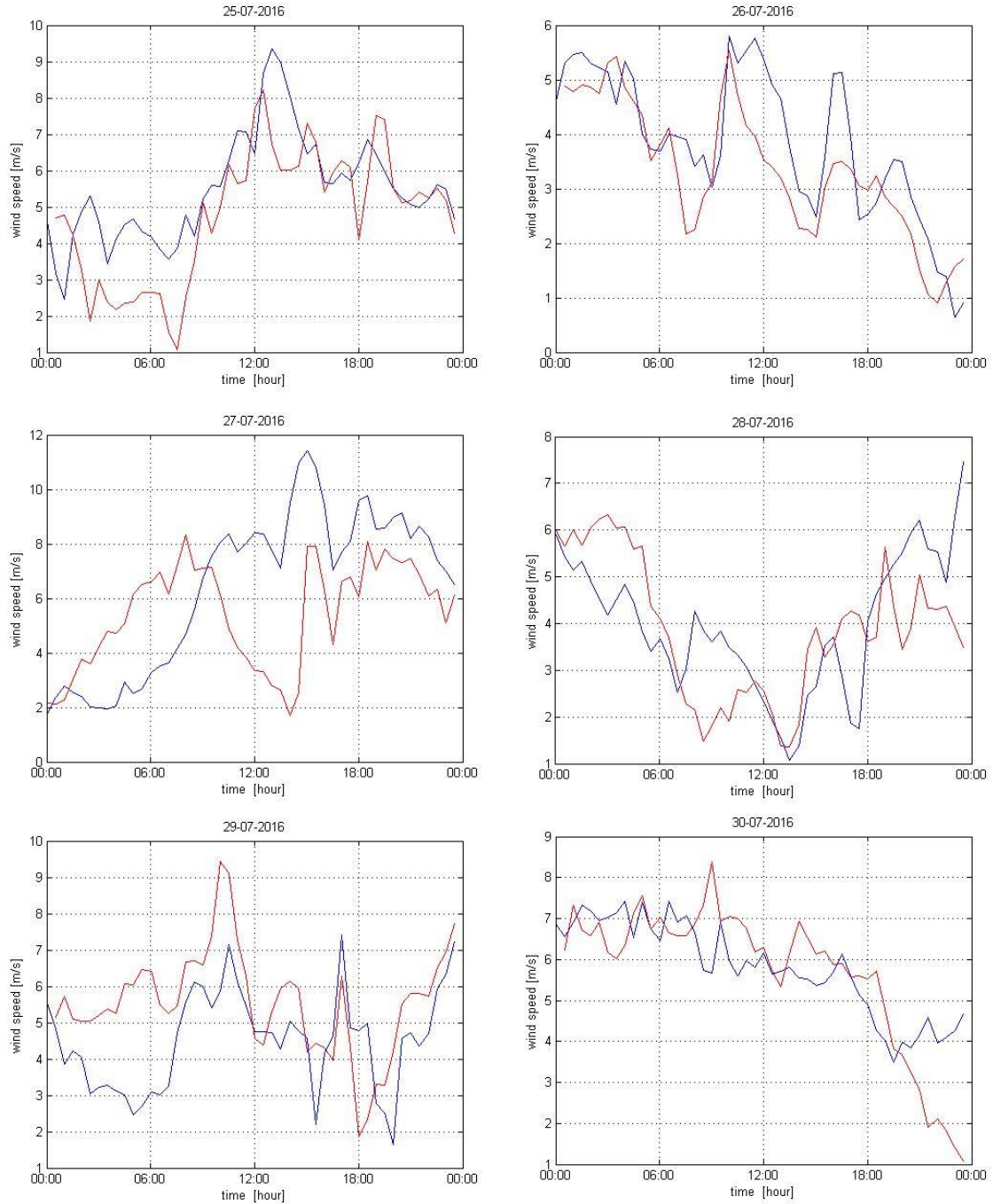


Figure A.7: Wind speed over time for the days 25 – 26 – 27 – 28 – 29 – 30 July 2016. The red line represents the 10-min average value measured with the lidar; the blue one corresponds to the simulation data (30-min value).

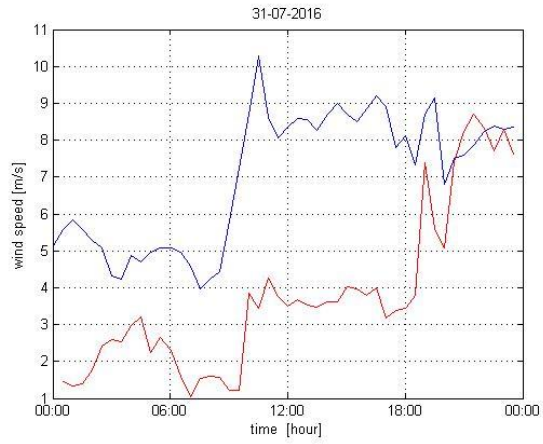


Figure A.8: Wind speed over time for day 31 July 2016. The red line represents the 10-min average value measured with the lidar; the blue one comes from the simulation data (30-min value).

Appendix B – Results for the FINO1 campaign

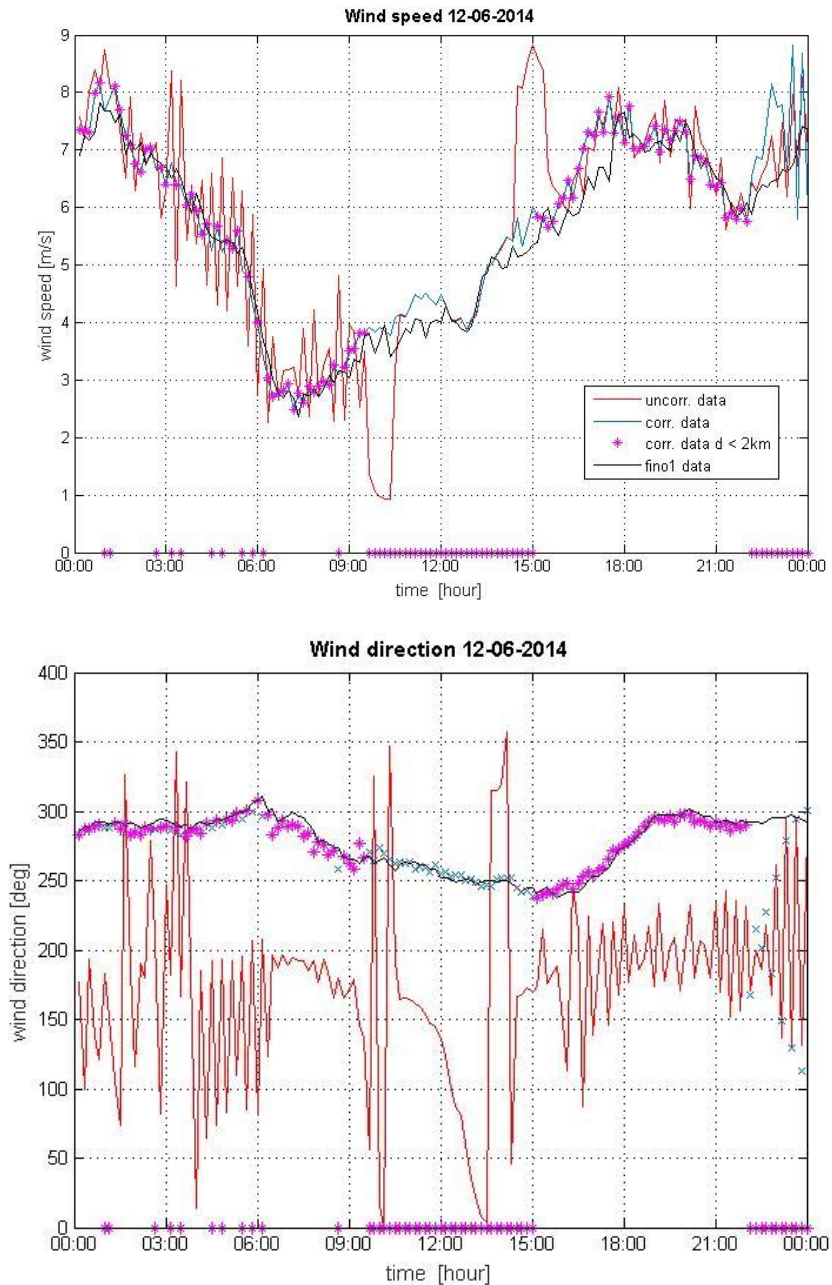


Figure B.1: Wind speed for the sample day 12 June 2014. The red line represents the wind speed value measured with the lidar before the correction has been applied; the blue one corresponds to the corrected lidar data (10-min average); the black line corresponds to the FINO1 wind speed and the pink one represents the corrected lidar data only when the ship is close to the met. mast (distance $d < 2$ km; when the distance is bigger than 2 km, a dummy zero value is shown).

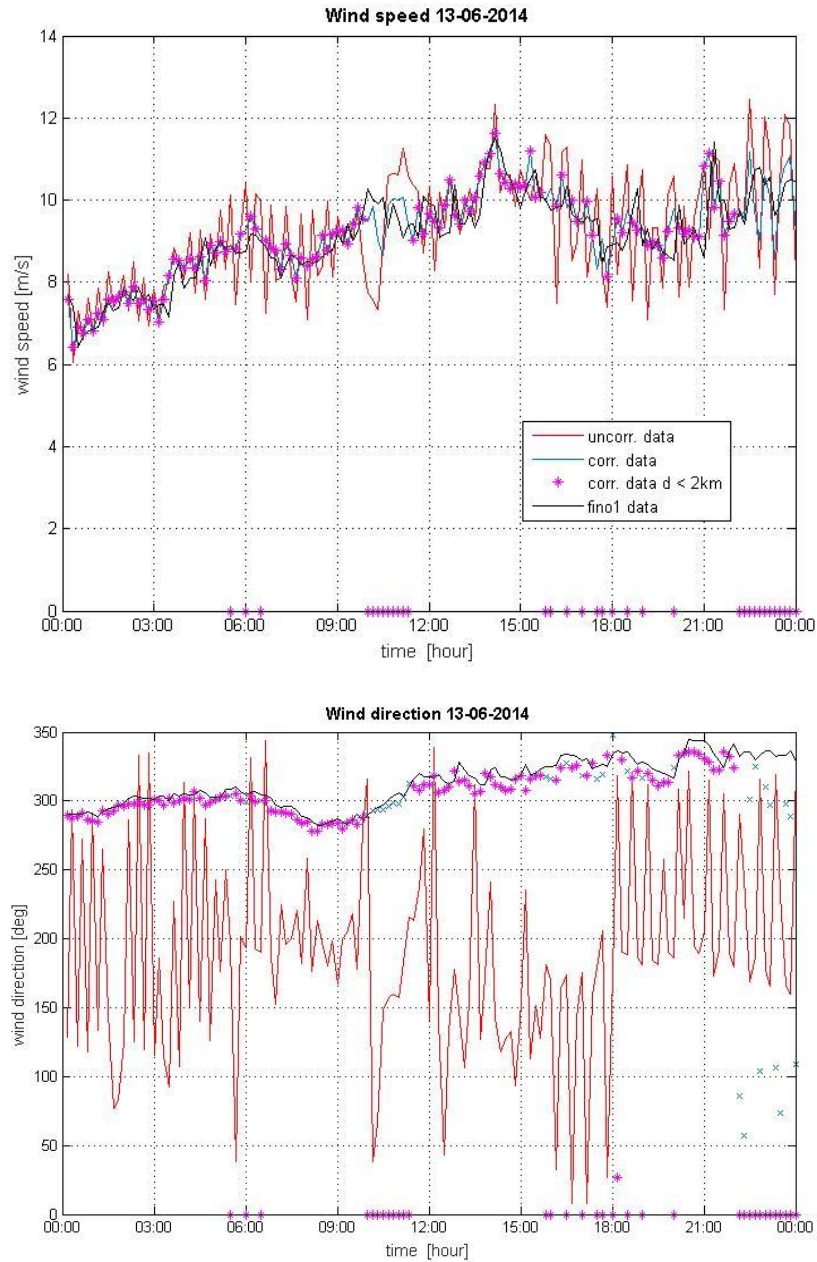


Figure B.2: Wind speed for the sample day 31 June 2014. The red line represents the wind speed value measured with the lidar before the correction has been applied; the blue one represents the corrected lidar data (10-min average); the black line corresponds to the FINO1 wind speed and the pink one represents the corrected lidar data only when the ship is close to the met. mast (distance $d < 2$ km; when the distance is bigger than 2 km, a dummy zero value is shown).

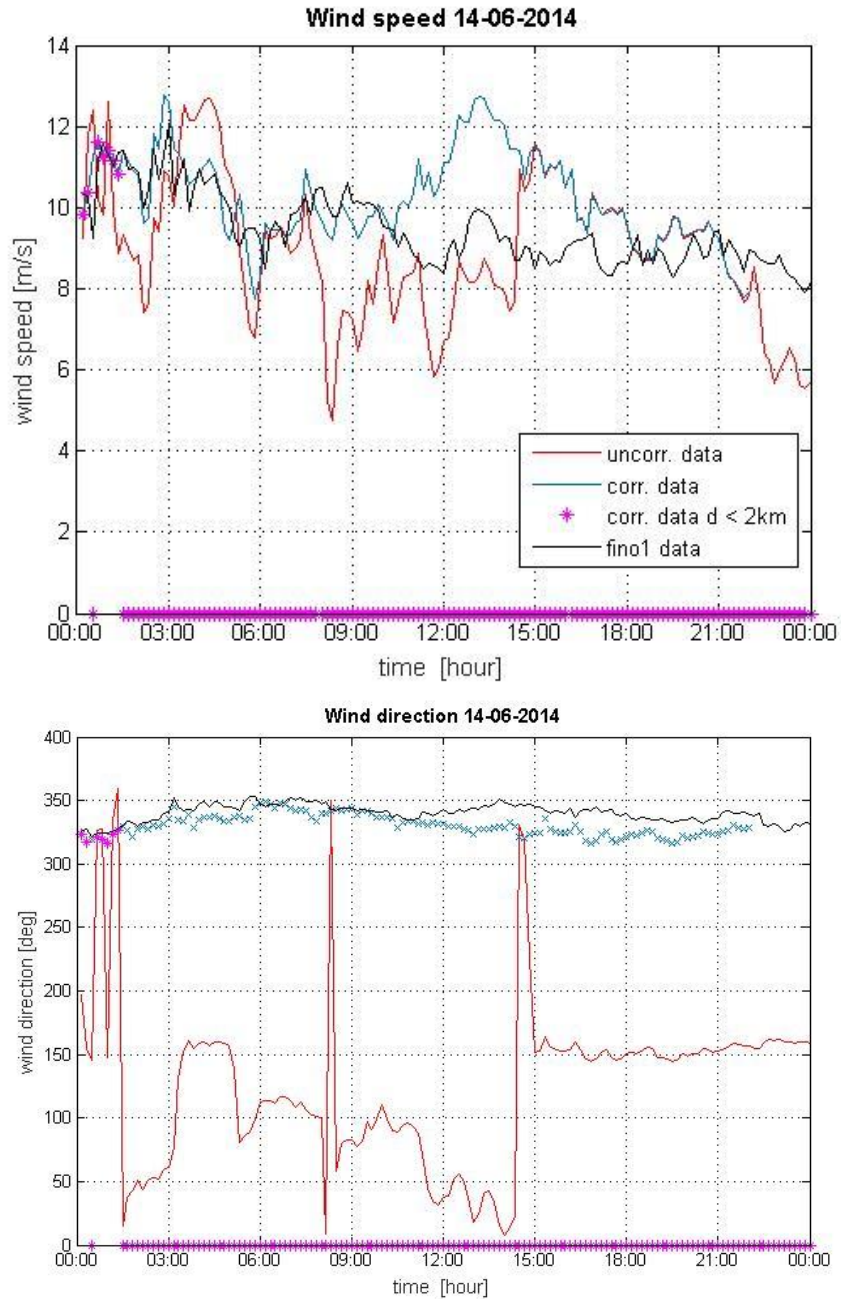


Figure B.3: Wind speed for the sample day 14 June 2014. The red line represents the wind speed value measured with the lidar before the correction has been applied; the blue one represents the corrected lidar data (10-min average); the black line corresponds to the FINO1 wind speed and the pink one represents the corrected lidar data only when the ship is close to the met. mast (distance $d < 2$ km; when the distance is bigger than 2 km, a dummy zero value is shown).